1988

Mechanical-chemical energy transfer observations of vaporific explosions.

Rodriguez, Gilberto

NAVAL POSTGRADUATE SCHOOL
Monterey, California

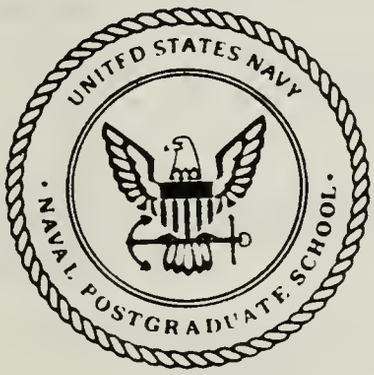

THESIS

MECHANICAL-CHEMICAL ENERGY TRANSFER
OBSERVATIONS OF VAPORIFIC EXPLOSIONS

by

GILBERTO RODRIGUEZ

JUNE 1988

THESIS ADVISOR: G. F. KINNEY

RITY CLASSIFICATION OF THIS PAGE

REPORT DOCUMENTATION PAGE

EPORT SECURITY CLASSIFICATION CLASSIFIED	1b RESTRICTIVE MARKINGS
ECURITY CLASSIFICATION AUTHORITY	3. DISTRIBUTION / AVAILABILITY OF REPORT Approved for public release; distribution is unlimited
ECLASSIFICATION / DOWNGRADING SCHEDULE	
RFORMING ORGANIZATION REPORT NUMBER(S)	5 MONITORING ORGANIZATION REPORT NUMBER(S)
AME OF PERFORMING ORGANIZATION al Postgraduate School	6b OFFICE SYMBOL (If applicable) 61KY
	7a. NAME OF MONITORING ORGANIZATION Naval Postgraduate School
DDRESS (City, State, and ZIP Code) nterey, California 93943-5000	7b. ADDRESS (City, State, and ZIP Code) Monterey, California 93943-5000
AME OF FUNDING / SPONSORING RGANIZATION	8b. OFFICE SYMBOL (If applicable)
	9. PROCUREMENT INSTRUMENT IDENTIFICATION NUMBER
DDRESS (City, State, and ZIP Code)	10 SOURCE OF FUNDING NUMBERS

PROGRAM ELEMENT NO.	PROJECT NO.	TASK NO	WORK UNIT ACCESSION NO.

ITLE (Include Security Classification)

CHANICAL-CHEMICAL ENERGY TRANSFER OBSERVATIONS OF VAPORIFIC EXPLOSIONS

ERSONAL AUTHOR(S)
driguez, Gilberto

TYPE OF REPORT	13b TIME COVERED	14. DATE OF REPORT (Year, Month, Day)	15 PAGE COUNT
ster's Thesis	FROM _____ TO _____	1988 June	60

UPPLEMENTARY NOTATION The views expressed in this thesis are those of the author d do not reflect the official policy or position of the Department of fense or the U. S. Government.

COSATI CODES			18 SUBJECT TERMS (Continue on reverse if necessary and identify by block number)
FIELD	GROUP	SUB-GROUP	Vaporifics

BSTRACT (Continue on reverse if necessary and identify by block number)

This study incorporates an experiment performed with the objective of panding the existing knowledge about "Vaporific Explosions". This enomenon, known to produce extensive damage to targets, is studied for a ssible energy transfer mechanism occurring during the projectile-target pact interaction. This investigation is concentrated mainly to observe the stribution and combustion of fragments (aluminum particles) within the fragnt beam and the transfer of kinetic energy to surfaces on the target. The sults indicated no evidence of combustion for the selected targets. The alysis of the closed target configurations showed that the main cause for mage was the transfer of kinetic energy to the surface within the target.

ISTRIBUTION / AVAILABILITY OF ABSTRACT UNCLASSIFIED/UNLIMITED ☐ SAME AS RPT ☐ DTIC USERS	21. ABSTRACT SECURITY CLASSIFICATION Unclassified
NAME OF RESPONSIBLE INDIVIDUAL F. Kinney	22b TELEPHONE (Include Area Code) (408) 646-2107
	22c OFFICE SYMBOL 61KY

ORM 1473, 84 MAR 83 APR edition may be used until exhausted
All other editions are obsolete

SECURITY CLASSIFICATION OF THIS PAGE

☆ U.S. Government Printing Office: 1986—606-243

Approved for public release; distribution is unlimited

Mechanical-Chemical Energy Transfer Observations of Vaporific Explosions

by

Gilberto Rodriguez
Captain, United States Army
B.S., University of Puerto Rico, Cayey, 1980

Submitted in partial fulfillment of the
requirements for the degree of

MASTER OF SCIENCE IN PHYSICS

from the

NAVAL POSTGRADUATE SCHOOL
June 1988

ABSTRACT

This study incorporates an experiment performed with the objective of expanding the existing knowledge about "Vaporific Explosions". This phenomenon, known to produce extensive damage to targets, is studied for a possible energy transfer mechanism occurring during the projectile-target impact interaction. This investigation is concentrated mainly to observe the distribution and combustion of fragments (aluminum particles) within the fragment beam and the transfer of kinetic energy to surfaces on the target. The results indicated no evidence of combustion for the selected targets. The analysis of the closed target configurations showed that the main cause for damage was the transfer of kinetic energy to the surface within the target.

TABLE OF CONTENTS

LIST OF TABLES

LIST OF FIGURES

ACKNOWLEDGEMENT

This work owes much to the many people who have offered generously their time and experience. Without their generosity the completion of this work would have been definitely more difficult.

The experience and technical assistance of Mr. Steve Finnegan, Mr. Kenneth Pringle and Mr. Kenneth J. Graham were invaluable. The advise and support of Mr. Mark Alexander, Mr. Robert G. S. Sewell and Mr. Marvin Backman were always welcome.

Finally, I am most grateful to Professor Gilbert F. Kinney who laid the ground work for my interest in this area and for his guidance and expertise.

I. INTRODUCTION

Projectiles with sufficient kinetic energy to perforate a target and form small fragments, can produce an effect known as "VAPORIFIC". The term vaporific was first used in 1947 by Dr. John S. Rinehart and Morgan G. Smith at the New Mexico School of Mines, during the course of a series of experiments which required the firing of 1/4 inch steel cubes against an aircraft [Ref. 1]. This definition was used to explain the explosive-like effect that caused extensive structural damage to the aircraft when attacked by the 1/4 inch steel cubes. Dr. Rinehart suggested that the nature of this effect can be attributed to the very rapid burning of aluminum vapor developed during the impact of the steel projectile against the aircraft structure. He thought the damage was so terrific that he named it "VAPORIFIC".

Since vaporific damage was first observed, more than twenty five years ago, a fair amount of research has been done by different research agencies throughout the United States and United Kingdom [Ref. 1, 2]. Research had been designed mainly toward obtaining information on some of the more important aspects involved in the process and to gather firm evidence on the damage incurred. Reports, as early as 1950, indicate that the effect was well demonstrated, particularly against aircraft [Ref. 3, 4]. Later research

was directed more to the understanding of the mechanism involved in what is clearly a very complex process.

While earlier studies demonstrated the high damage potential of the vaporific effect, little information was available regarding the explosive impact explanation of vaporific damage. Reports describing early work were hard to obtain and some investigative work was never published. Originally, the effect was thought to be an impact energy induced chemical reaction in which a form of aluminum metal vapor suffered a rapid oxidation reaction. This definition prevailed for a period of years until the phenomenon was observed to produce the same damaging effects in inert gas atmosphere and simulated altitude tests. Subsequent studies confirmed that the vaporific damage is a combination of chemical and mechanical processes. For this thesis an experiment was designed to attempt to separate the two events taking place in vaporific explosions. Since rapid oxidation of particles and kinetic energy capture are the dominant theories describing the phenomenon, by varying the particle sizes and keeping the speed in the ultra to hypervelocity range, a possible transition between mechanical and chemical events may be observed, under the assumption that there is a critical size for which the particles will produce one event more than the other.

II. BACKGROUND

Around 1950 investigative work began in the Naval Ordnance Test Station, China Lake, California to determine the feasibility of using this type of explosive effect as a kill mechanism in missile warheads [Ref. 2, 3]. Using a shaped charge at long standoff, it was found that an aircraft seemed to explode from internal blast when struck by the high velocity jet. The damage produced to the target was so devastating that it caught the immediate attention of researchers. Further research programs were established to study the effects of vaporifics and to conduct theoretical analysis of the results to supplement the existing knowledge of vaporific blast and its effects.

To adequately describe vaporific damage, new theories were developed and a series of experiments were conducted. A couple of hypotheses were tested concurrently with the experiments. One hypothesis was that vaporific damage was the result of high velocity objects impacting a target and breaking up in small finely divided particles. These particles then, in the presence of an oxidizer (air), and the temperature generated by the impact, will produce a dust type explosion. Another hypothesis stated that the damage was the result of the loss of kinetic energy and work done

on the target at near impact point [Ref. 5]. Up to this time, these two hypotheses described the effect best.

To obtain a better concept of what was happening within a target and confirm previous theories, experiments were conducted using single pellets fired from the end of a cylindrical explosive charge. The pellets were made of a variety of materials including nickel, steel, and aluminum. They were projected at speeds between 2500 and 4800 meters per second against simple box-like structures built of aircraft materials. Some of the targets were filled with gases such as helium, nitrogen, oxygen, and engine exhaust gases. The purpose was to determined whether or not the effect was purely chemical. The conclusion was that chemical processes were indeed part of the vaporific effect. It was also concluded that the flashing characteristics were suppressed by inert atmosphere and enhanced by air or oxygen rich atmosphere. The presence of nitrogen increased extensively the amount of damage incurred to the target.

Similar studies were conducted by the Ballistic Research Laboratory, Aberdeen, Maryland. In these studies, single spherical and cubical projectiles were fired by means of sabots through thin aluminum entrance plates into a chamber instrumented with pressure gauges. Calculations of the pressure rise were performed by determining the striking and exiting velocities of the fragment, assuming that the lost energy was expended entirely in heating the air in the

chamber. Calculated pressures were then compared to observed pressures. The comparison of pressures indicated a small rise in pressure suggesting that an additional energy must be present, such as the energy release from the combustion of aluminum.

As mentioned earlier, previous tests suggested that the vaporific damage was caused by oxidation of the aluminum and therefore, it would be reduced with altitude, where the oxidizer content would be less. Work done at the Naval Weapons Center, China Lake, regarding altitude effect on shaped charges, provided a very interesting aspect of the vaporific effect. The damage effect was observed to increase with altitude rather than be reduced as would be expected. The results produced, for the first time, evidence that the damage producing effect was not all chemical. In fact, analysis of the results showed the main cause of damage was mechanical. The terminal effects on the target were evidently the same as at lower altitude. The results showed that the principal mechanism for the damaging effect can be attributed to reduced air drag on the small particles which result in less velocity reduction. The consequences are that fragments reach higher velocities and produce more shock and kinetic energy transfer.

A report by Lawrence N. Cosner and John Pearson, "The Cross-Wind Firing of Large Shape Charges", presented another interesting aspect [Ref. 5]. The damage produced to the

target was enhanced by the smearing effect of the jet. A couple of years before this experiment a description of the jet, after the collapse process, was published by L. N. Cosner, R. G. S. Sewell and H. W. Wedaa [Ref. 3]. In this report, they described the jet as a composition of many hundreds or thousands of small particles ranging in size from microscopic to approximately 1/2 inch in diameter. Also as far as particles were concerned, three kinds of impact are present depending on whether:

1. Particle diameter is less than the target thickness.
2. Particle diameter is equal to the target thickness.
3. Particle diameter is greater than target thickness.

The bearing this has on the amount of vaporific damage may be quite important. It shows that particle size and distribution are important parameters for vaporific damage.

For the next several years, tests were conducted to exploit this phenomenon. Work was concentrated more to shaped charge attack of aircraft, aircraft engines, propellers, etc. The outcome of these experiments provided a lot of information about the vaporific effect. A few of the reports presented thermodynamic analysis and others concentrated on shock, energy degradation, and somewhat less on kinetic energy transfer. All of these parameters occur in a very short time, and are manifested in a form equivalent to an explosive energy release. A more exact description or explanation of the mechanism involved in the

vaporific explosion does not exist at the present. However, an exact definition of vaporific explosions and its causes and effects can be found, as it is the purpose of this work. Research is still being conducted, but dissemination of the information is minimal.

III. EXPERIMENT

Figures 1 and 2 show a schematic representation of the experimental setup. The capsule projector used was a 0.50 caliber, smooth bore, evacuated-chamber powder gun. The system was limited to a top speed of approximately 2800 meters per second, beyond this, velocity equipment damage may occur. Velocities of the capsule projectile were measured at the muzzle with a photodiode system coupled to an interval counter. The distance between the photodiodes was 0.266 meters. The muzzle of the gun was sealed with a mylar sheet and a vacuum pump was used to evacuate the chamber. This measure prevents the interruption of the projectile flight by the expanding gases of the burning propellant.

Running these tests required a projectile made of material sufficiently strong not to disintegrate, melt or burn while in flight, but soft enough to break easily upon impact and that will not contribute large fragments to the dispersing particles. A gelatine capsule proved to be adequate for our purpose. Each projectile was composed of aluminum powder enclosed in a gelatine capsule. The capsule was then placed in a fly-apart, polycarbonated sabot.

Aluminum powder was selected as the main filler for the projectile for two reasons. First, previous reports

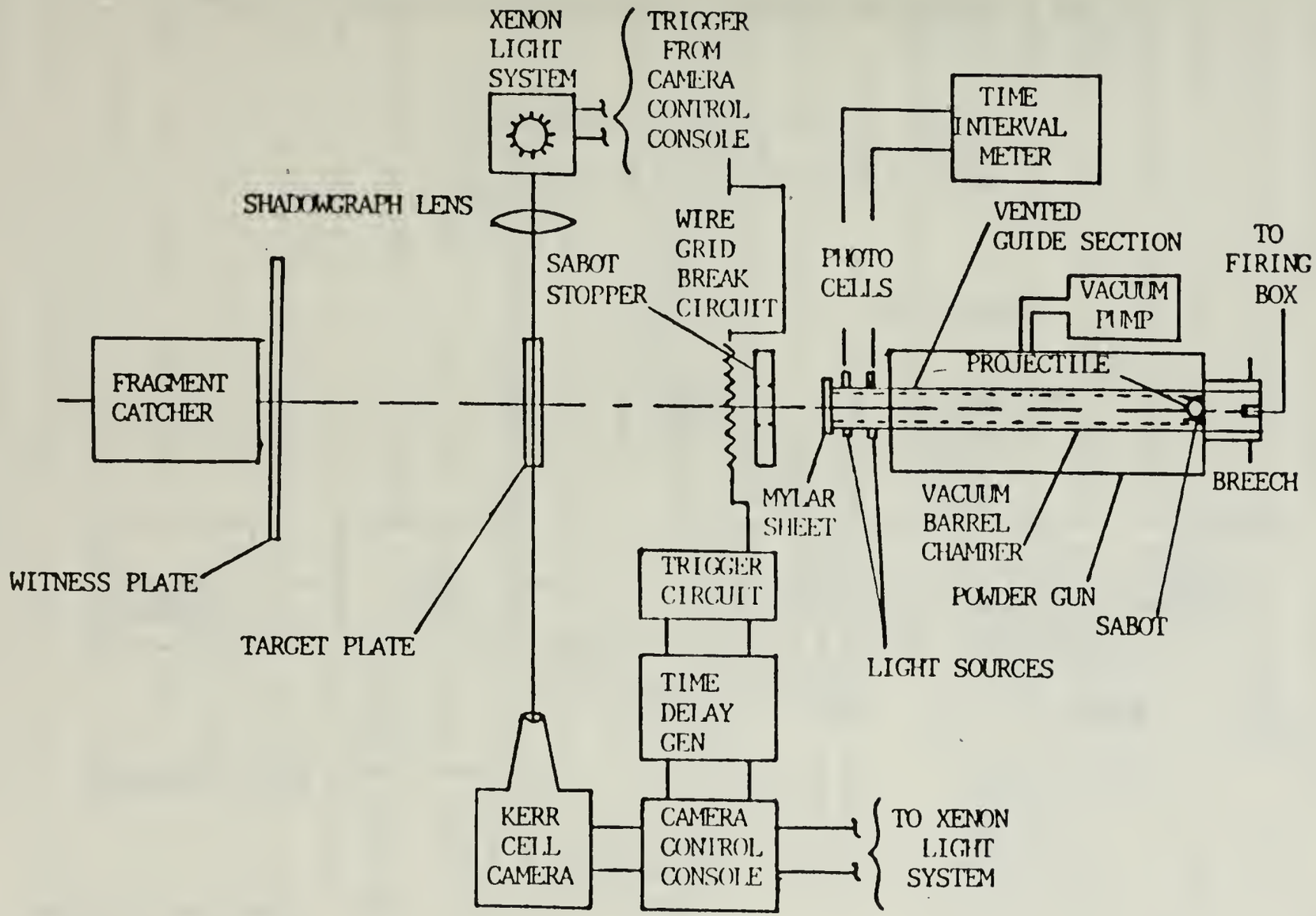

Figure 1 Test Setup Schematic Diagram for Tests 1-4

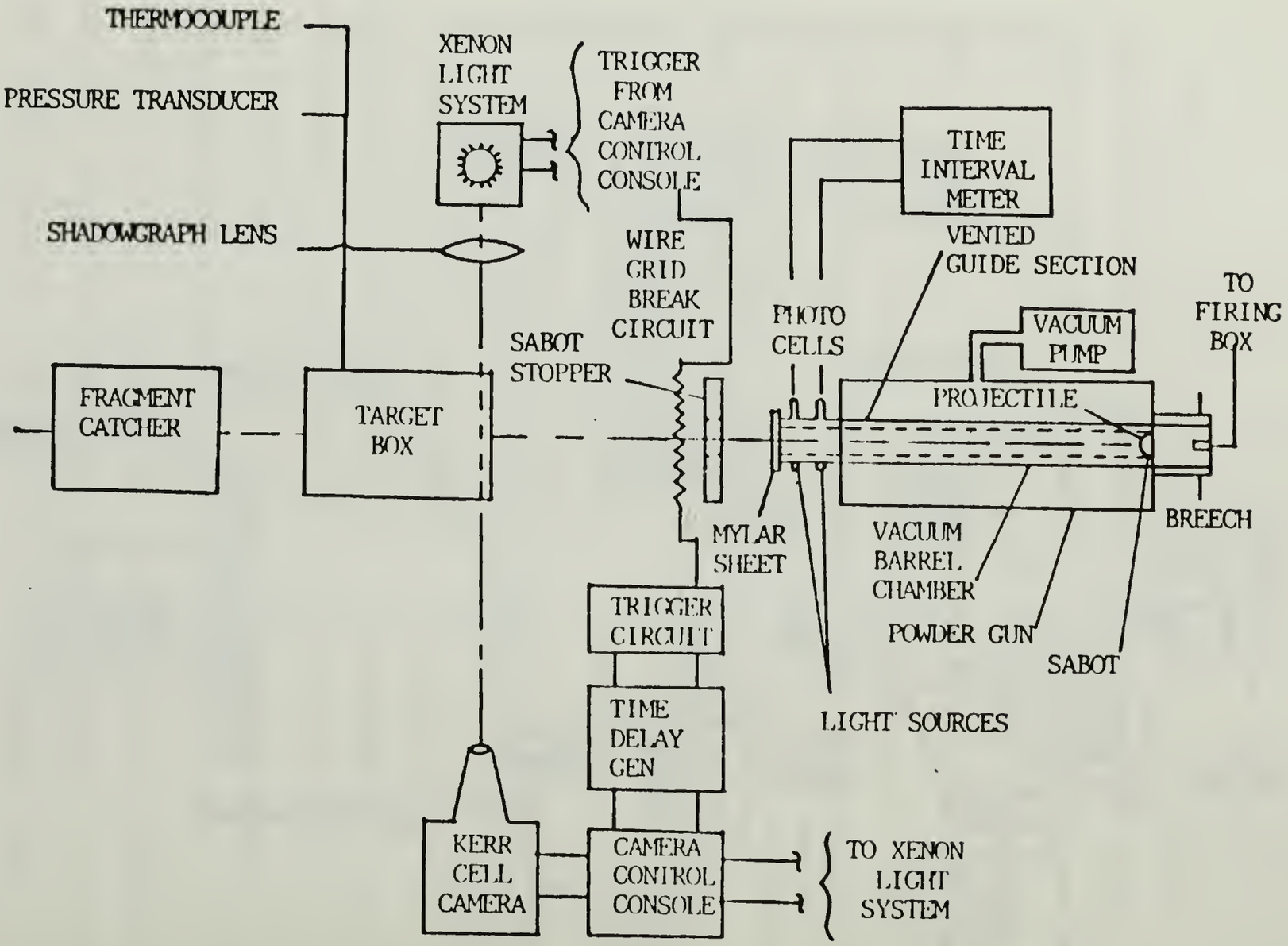

Figure 2 Test Setup Schematic Diagram for Tests 5 and 6

indicated that the majority of the experiments performed utilized some sort of aluminum related metal as the impact target and to some extent, as the projectile. Second, aluminum was a readily available powder metal for which particle size was known. Since part of this work is to separate the transition between mechanical and chemical effect, knowing the particle size increased the possibilities of obtaining a range of sizes for which the transition can be observed.

The sabot was separated from the projectile by the air friction and stopped by the sabot stopper. The sabot stopper was a heavy steel plate with a hole drilled through the center. This plate was located about 91.5 centimeters downrange from the gun muzzle. The hole size was made to allow the capsule to pass through and at the same time to trap the rapidly diverging sabot sections.

Experimental evidence was obtained using a Kerr Cell photographic system. To activate the system a wire grid break circuit placed in front of the target was used. Once the projectile passes through the sabot stopper, breaking the continuity of the circuit, it will trigger the Xenon lights and the Kerr Cell camera. The timing between frames was selected by means of a digital timer connected to the circuit. As a reference scale, a caliper with a preset measure of 3.81 centimeters between tips was used.

Target, in this thesis, is defined as the immediate area surrounding the projectile impact point. Two types of targets were used. The first targets employed were glass plates 0.1 centimeter thick and 80.0 centimeters in area. These plates were wrapped with tape to prevent large glass fragments mixing with the aluminum particles. Each of these plates were then attached to a frame plate of dimensions, 30.5 centimeters in length by 30.5 centimeters width, with a hole in the center of 4.0 centimeters in diameter as shown in Figure 3a.

The second set of targets were plates of 2024 T3 aluminum, 180.0 centimeters in area and thicknesses of 0.05 centimeters. They were held in place in the same manner as the glass plates. These targets were selected thin, but hard enough to break the gelatine capsule and allow the aluminum particles to be dispersed in a metal to metal impact manner. Aluminum at standard atmosphere is coated with a natural layer of oxide. This coating is believed to be lost during metal to metal impact, increasing the possibilities of aluminum particle combustion. Taking this into consideration, relatively hard aluminum targets were utilized, instead of glass, for this part of the experiment. All targets were aligned along the central axis of the flight path of the projectile. This alignment assured normal or very low impact angles.

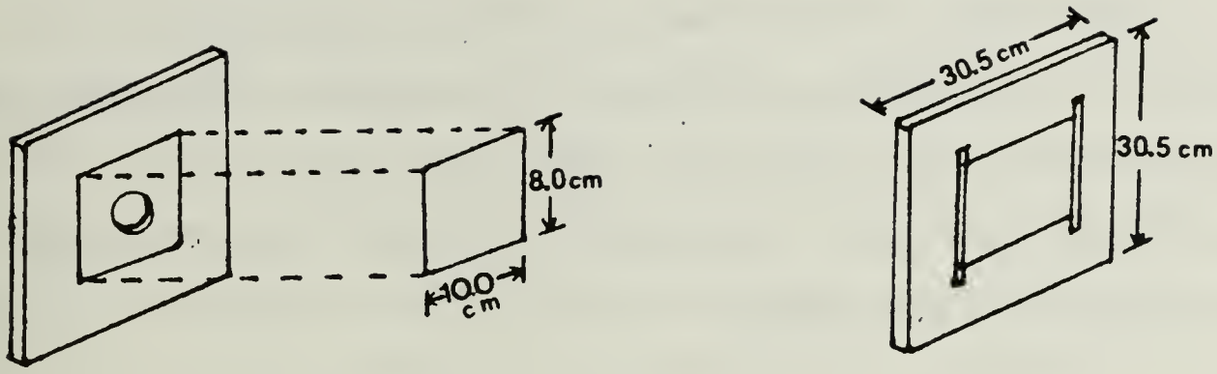

(a)

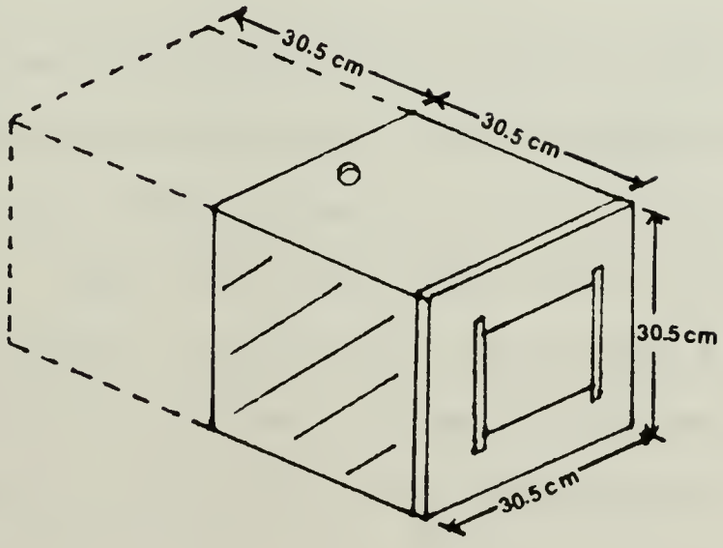

(b)

Figure 3 Target Configurations

A witness plate followed by a celotex fragment catcher was placed behind the targets and target boxes. Packaging paper was used for the first two tests. Plexiglass proved to be more adequate and was used for the remainder of the tests. The purpose was to observe the particle distribution pattern and to prevent the further traveling of the particles inside the laboratory that could cause fire and damage to other equipment.

IV. PROCEDURE

The experiment consisted of six different tests, all performed with the equipment previously described. Table I summarizes all tests performed. The basic experimental procedure was to fire the projectile at speeds around 2500 meters per second against different target configurations. For the first four tests, the configuration consisted of a target plate held to the open atmosphere and a witness plate located behind the targets. Distances for the witness plates are given in Table I. This arrangement provided an easy way to monitor and study the distribution and possible chemical reaction produced by the particles at high velocities.

The projectiles were fired with aluminum powder as the filler. The powder was selected to be of different grain sizes for each test. The average size used in each test is given in Table I. Once the projectiles were put together, they were fired against the targets, previously described. The different distances between target and witness plate allowed the study of the particle distribution well after impact.

The remaining two tests were performed in the same manner as before. The projectiles were filled with aluminum powder with a particle size of 95 microns. The target

TABLE I SUMMARY OF TESTS PERFORMED

TEST #	DATE M/Y	TARGET	DISTANCE TO TARGET (M)	PROJECTILE	POWDER TYPE /GRAIN SIZE (MICRONS)	PROJECTILE SPEED (M/S)	PROJECTILE WEIGHT (KG)	COMMENTS
1	9/87	GLASS PLATE	1.35	GELATINE CAPSULE CONTAINING ALUMINUM POWDER	H-5	2414.7	0.0018	KERR CELL CAMERA WITNESS PLATE (WP) DISTANCE 32.31 CM
2	9/87	"	"	"	H-30	2382.8	0.0020	KERR CELL CAMERA WITNESS PLATE DISTANCE 30.80 CM
3	9/87	"	"	"	H-60	2312.1	0.0019	KERR CELL CAMERA WITNESS PLATE DISTANCE 32.54 CM
4	9/87	2024-T3 ALUMINUM PLATE .041 CM THICK	"	"	H-95	2340.2	0.0022	KERR CELL CAMERA WITNESS PLATE DISTANCE 32.86 CM
5	1/88	"	"	"	"	2229.9	"	PRESSURE TRANSDUCER THERMOCOUPLE NO WITNESS PLATE
6	1/88	"	1.09	"	"	2285.4	0.0021	"

configuration was changed to simulate a closed compartment. A piezoelectric crystal type transducer rated for 15.0 PSI and a type K thermocouple were used. The reason for using these gauges was to obtain a rough estimate of how the pressure and temperature were changing within the compartment. The calibration history sheet for the pressure gauge and temperature-emf sheet for the thermocouple are provided in Appendices A and B. This setup was necessary to compare pressure and temperature changes and their contribution to the vaporific effect for different volumes. Both targets consisted of aluminum plates 0.1 centimeter thick attached to the box shown in Figure 3b, with the respective pressure transducer and thermocouple. The dashed line in the figure represents the added volume.

The box dimensions were 30.5 centimeters wide, 30.5 centimeters in length, and 30.5 centimeters in height. The last test used the same set up. However, the box length was increased to 61.0 centimeters. The reason for increasing the volume of the box was to study and compare the damage produced by the vaporific effect for compartments of different volume.

V. RESULTS

A. DATA COLLECTION AND REDUCTION

All information and raw data was obtained by means of photographs, visual inspection of the targets and witness plates, and voltage readings from a Nicolet oscilloscope connected to the pressure transducer and thermocouple. The distance between reference marks in the photographs is 3.81 centimeters. This distance was verified for consistency on every test. The dark line that appears in the photographs, is a piece of cotton string with a weight attached to it. It was used as a reference mark for the still picture camera. No other adjustments were neccessary for the photographs.

The data from the oscilloscope was in the form of voltage signals. A calibration history sheet, provided in Appendix A, was used to convert millivolts to pressure. For temperature changes, the tables in Appendix B give the thermoelectric voltage in absolute millivolts and the correspondent temperature in degrees centigrade. The reference temperature during the experiment was 20.0 degrees centigrade, which needs to be substracted from the temperature obtained from the table. No other adjustments were necessary.

B. EXPERIMENTAL RESULTS

The results discussed here are from a series of tests designed to study the overall interaction of the aluminum particles with the atmosphere surrounding the target, in this case, air. Since the purpose of this work is to study the possible causes producing the vaporific explosion, the idea of controlling the fragment (particle) size, provided the opportunity to observe the changes occurring to the fragment beam at very high speed. The only parameters allowed to vary were the initial impact velocity of the projectile and the fragment size. The masses of the projectiles varied less than one percent from each other, so they were assumed constant.

Figures 4, 5 and 6 show a series of high speed photographs of the projectile and target interaction. Also shown is the fragment beam profile. Fragment beam is referring to the cloud of particles formed after impact. They represent test numbers 1, 2 and 3 of the experiment. The time delay between frames is 15.0, 20.0 and 14.43 microseconds respectively. The camera was aimed from a different downrange distance to the target for each sequence of photographs. This allowed the observation of the fragment beam well after impact.

Figure 4 shows the sequence of photographs taken for test number 1. It was observed that the projectile retained its general shape, verifying that the gelatine capsule works

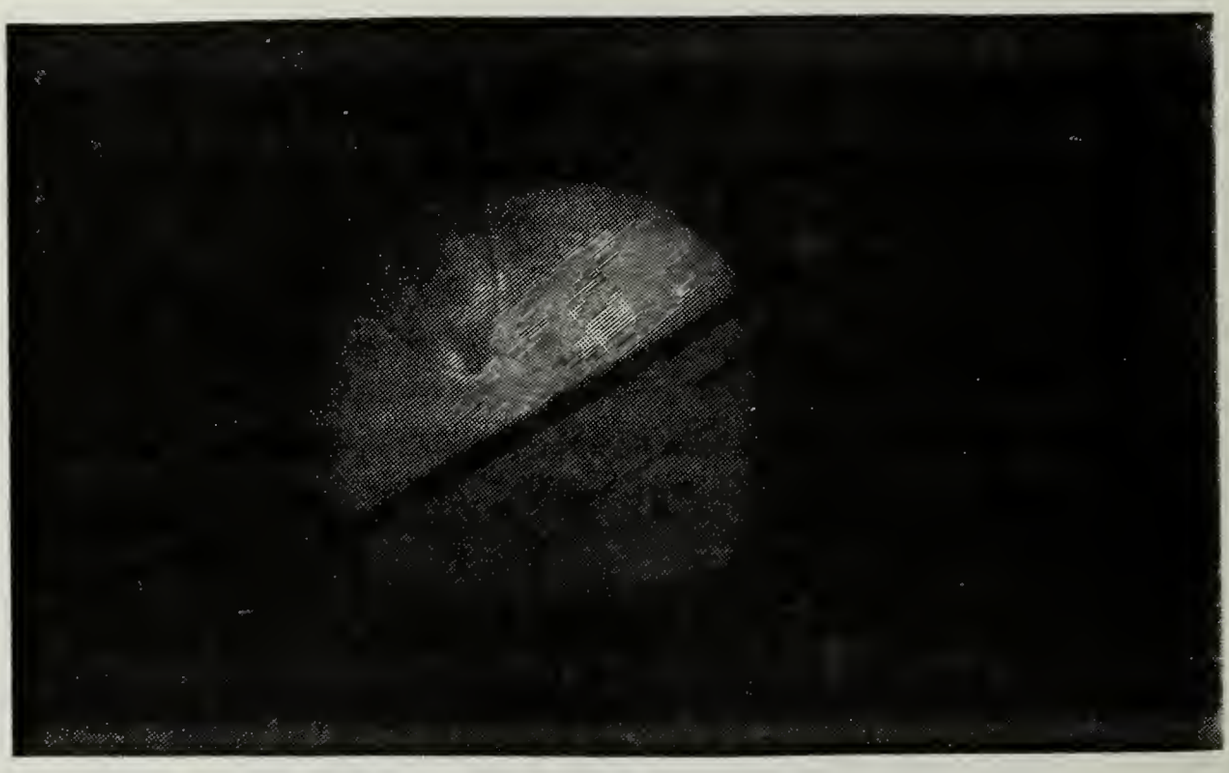

(a)

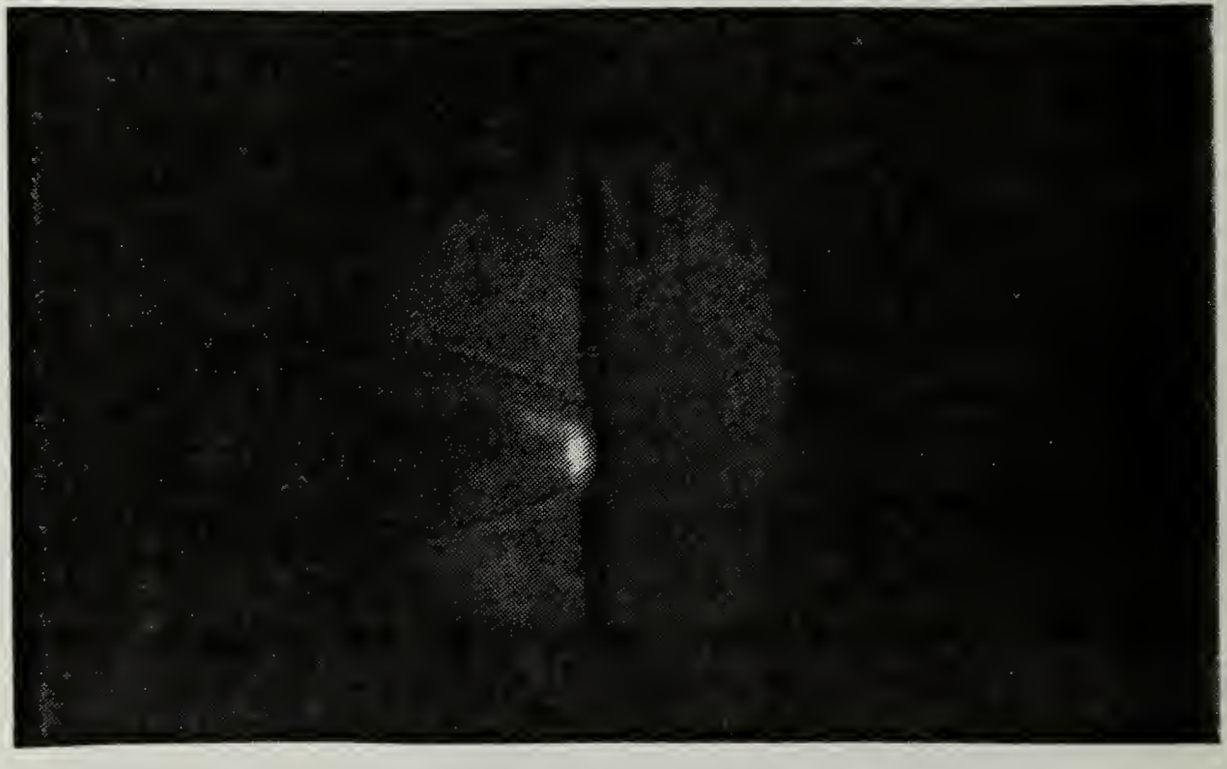

(b)

Figure 4 Sequence of Photographs for Test 1

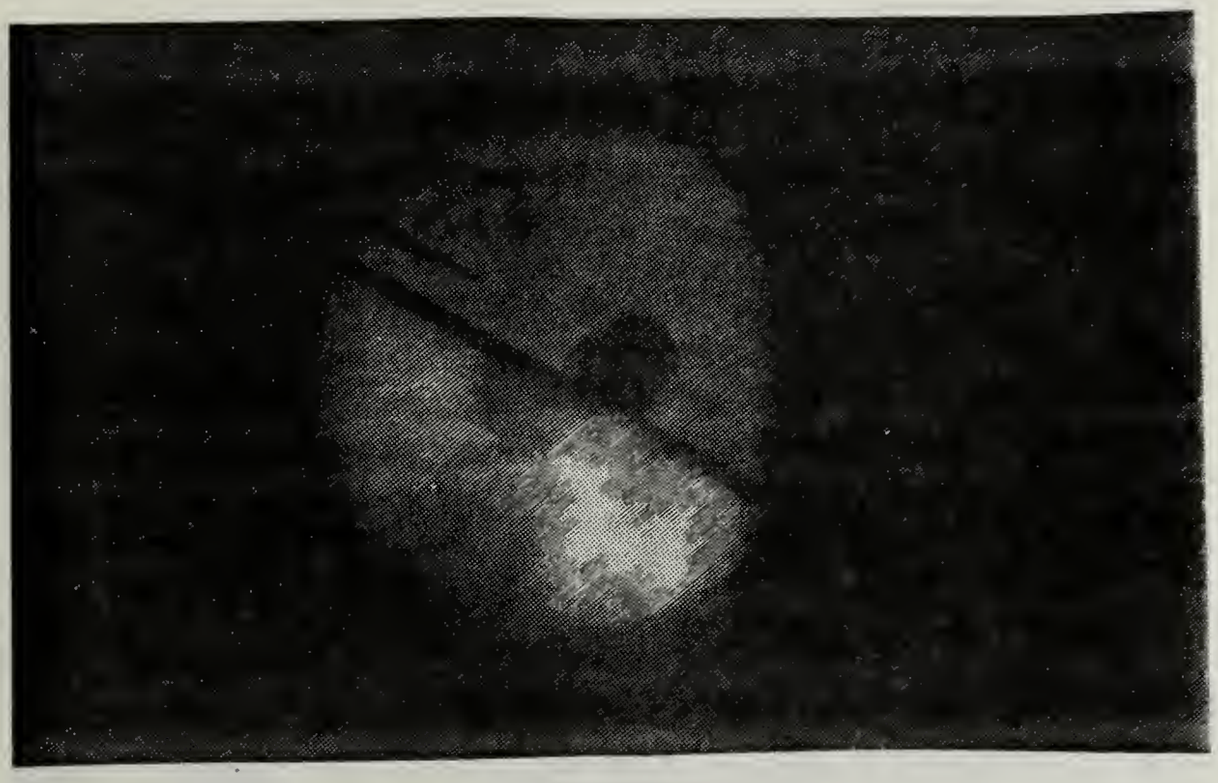

(c)

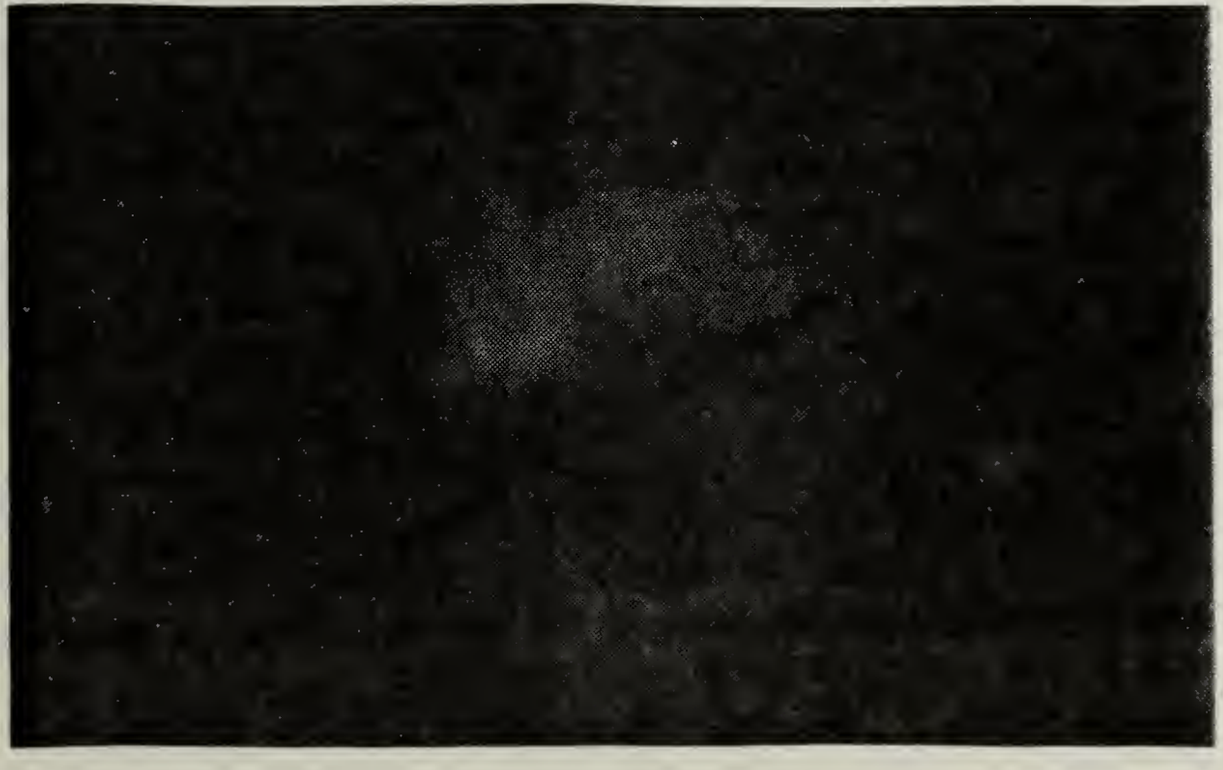

(d)

Figure 4 (Continuation)

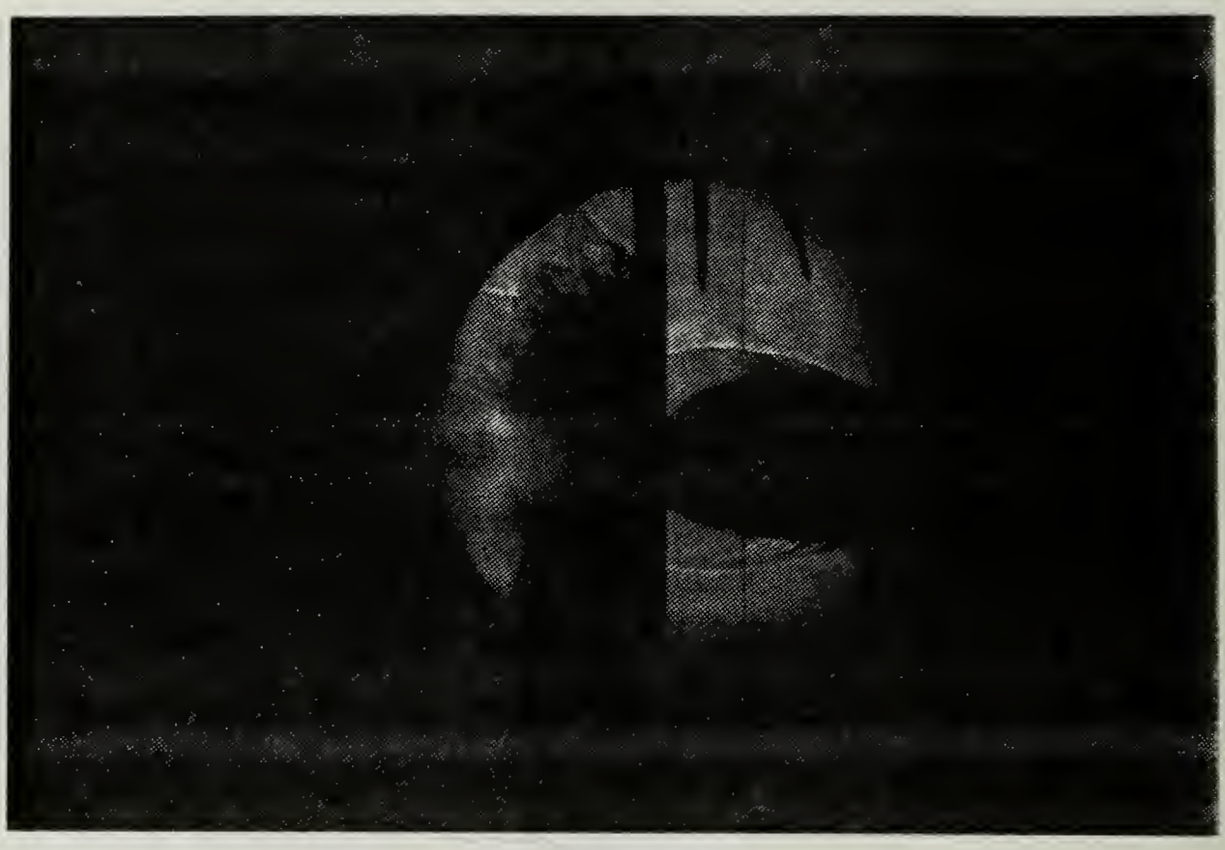

(e)

Figure 4 (Continuation)

well. A small deformation is noticed at the leading point of the projectile. This was attributed to the impact of breaking the mylar sheet used to seal the gun, or the passing of the projectile through the wire grid break circuit that triggered the Xenon light system. Note that in this sequence, the transformation of some energy into light is well appreciated. This is indicated by the bleaching of some areas of the photographs. Since the photographs were taken from a circular array of cameras, light was absorbed more easily in some of the photographs. These areas were

considered to be places where some type of combustion was taking place.

At impact, energy is transferred by means of friction and combustion to some of the materials involved. After impact, no clear areas are noticed. Combustion, or energy transfer of the same magnitude as before impact, is not evident in the fragment beam. Figure 5 also shows the presence of some type of combustion or energy transfer before impact, but none after impact, or within the fragment beam.

The witness plates for tests 1 and 2 were made of thick packaging paper. The heat generated by the impact of the fragment beam with the celotex fragment catcher produced a fire that partially destroyed both plates. The unburned portions left by the fire were studied and the only useful information obtained was that the fragment beam reached a diameter of approximately 18.0 to 20.0 centimeters for one of the plates. Since both were almost at the same distance behind the target, it was assumed that measurements of the diameter for both fragment beams varied very little.

Figure 6 shows the sequence of photographs for test number 3. Notice that the impact plate and target are not present. The reason is that the camera was aimed to capture the fragment beam well after the impact point. The large fragments that appeared in the photographs are the pieces of the polycarbonated sabot and target plate. The fragments

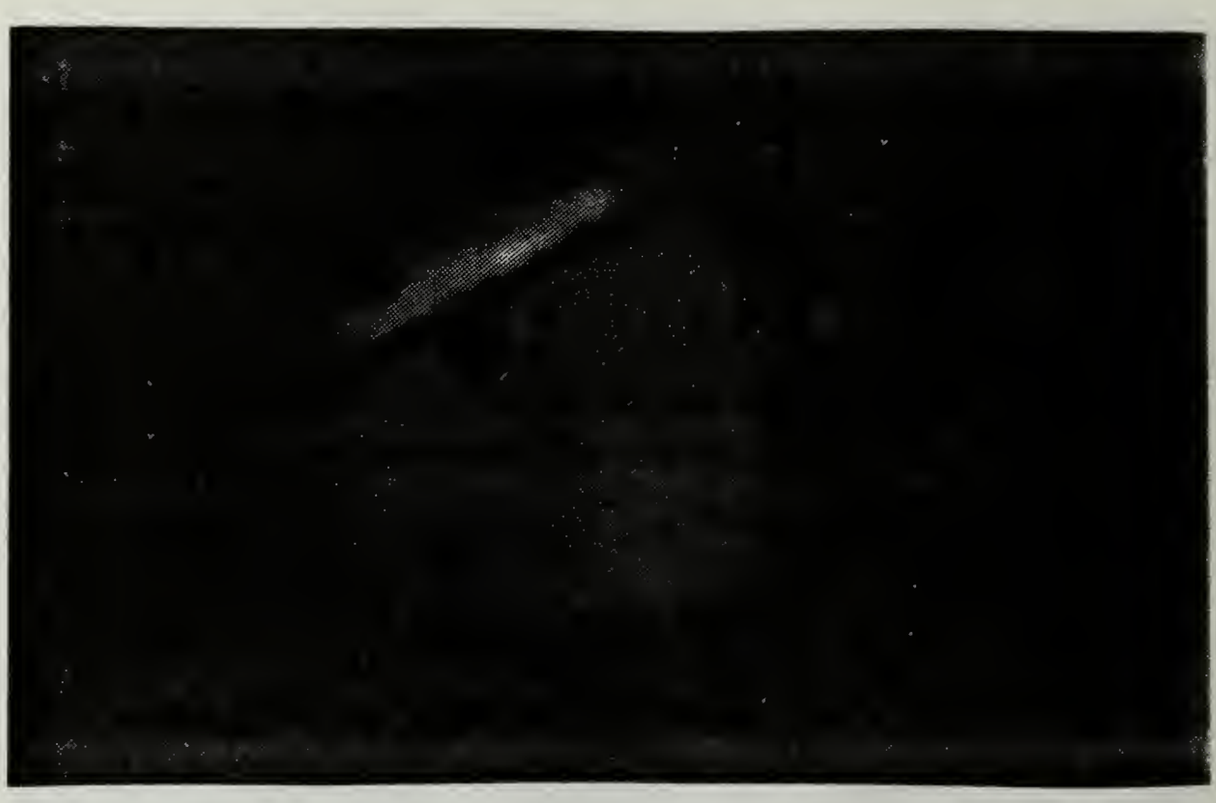

(a)

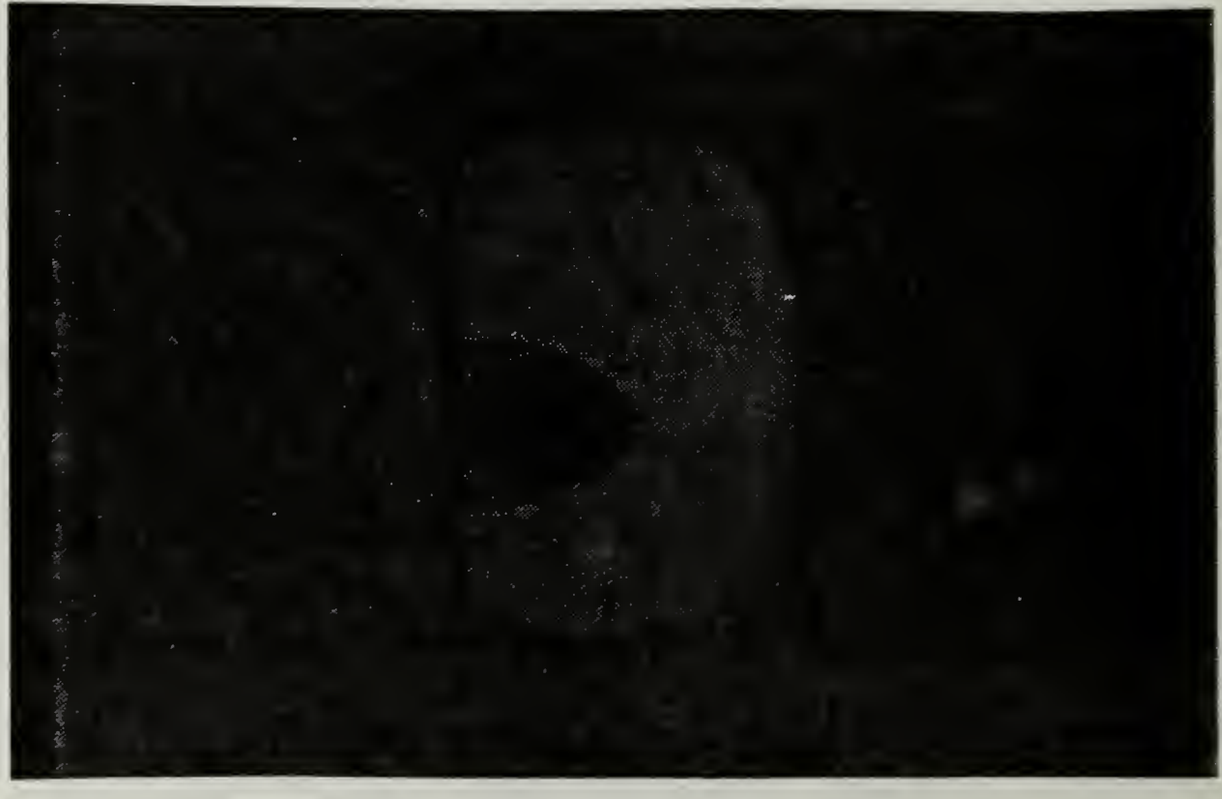

(b)

Figure 5 Sequence of Photographs for Test 2

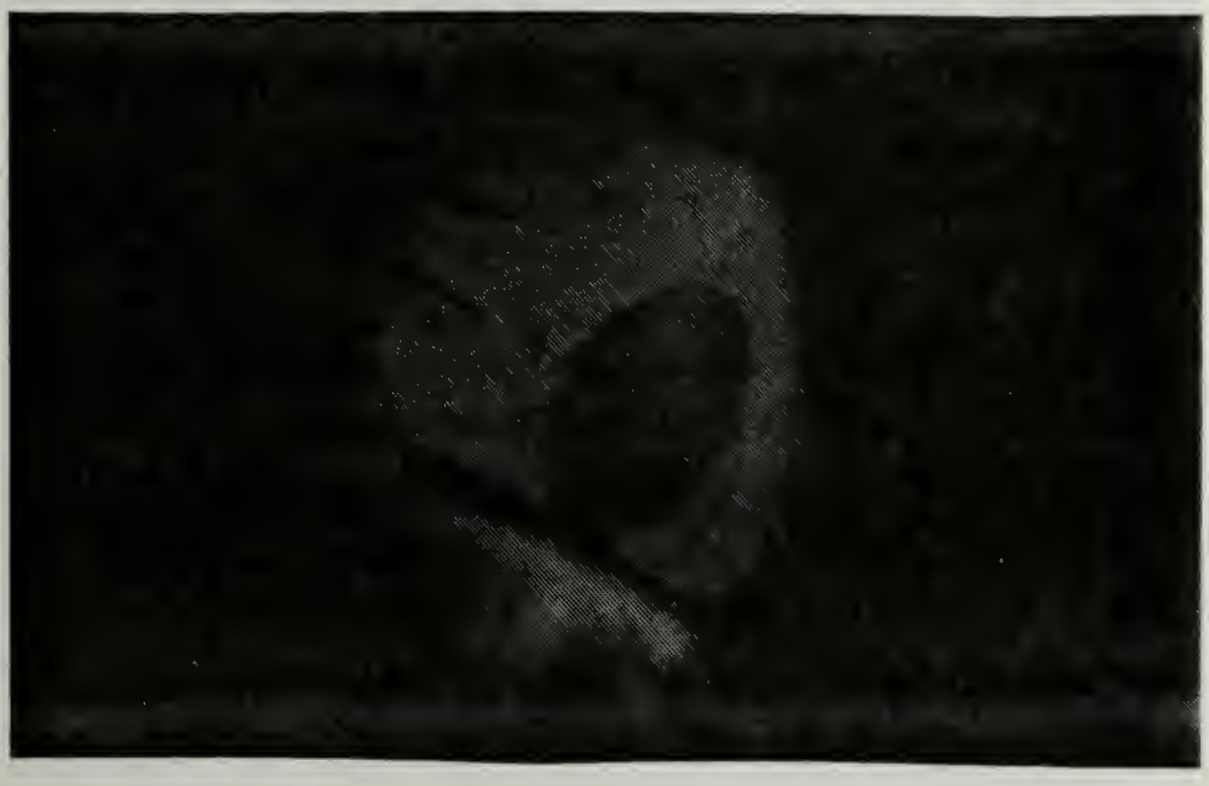

(c)

(d)

Figure 5 (Continuation)

(e)

Figure 5 (Continuation)

were produced by the impact of the sabot with the target. The reason being that it did not separate from the projectile early enough to be stopped by the sabot stopper. The time delay between impact and the first frame of the sequence was short for about 14.0 microseconds. This is the reason the first photograph does not show a fragment beam.

The unexpected large fragments appearing in this series of photographs revealed several interesting points. Individual particle shock waves can be observed and the larger fragments do not seem to be undergoing a combustion

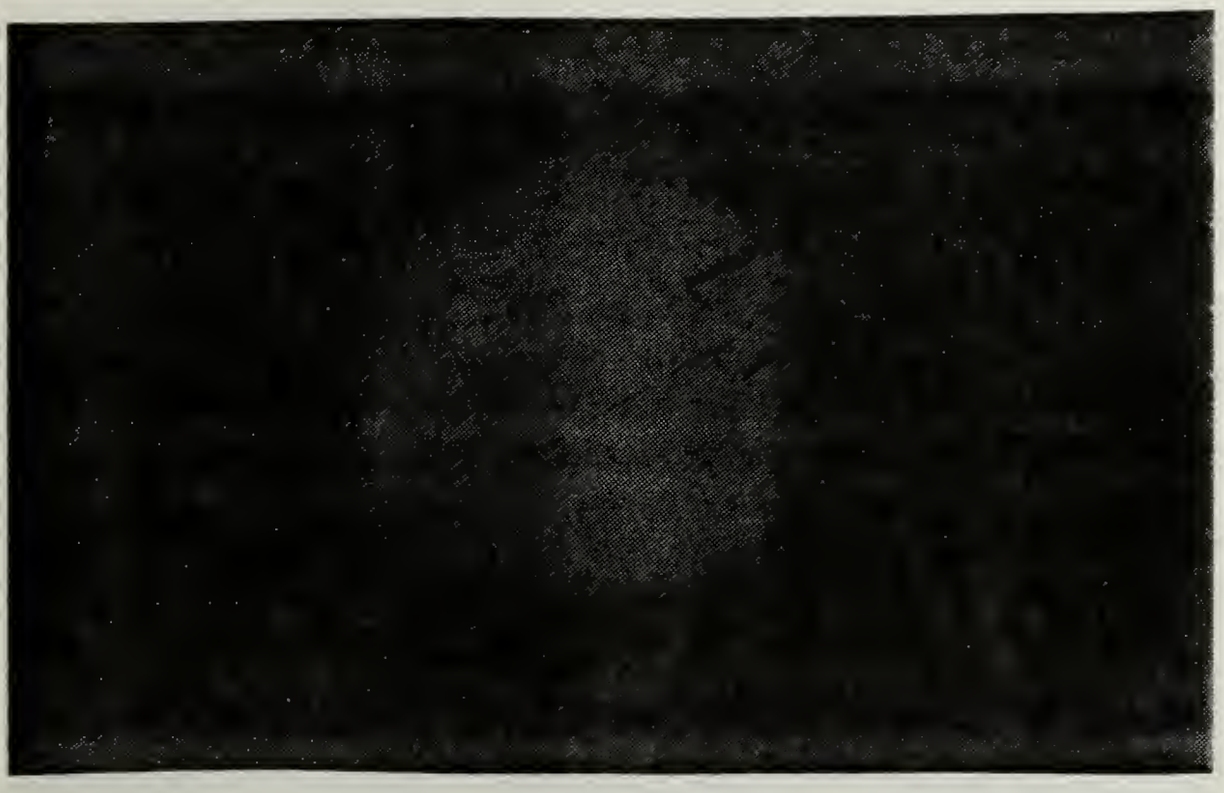

(a)

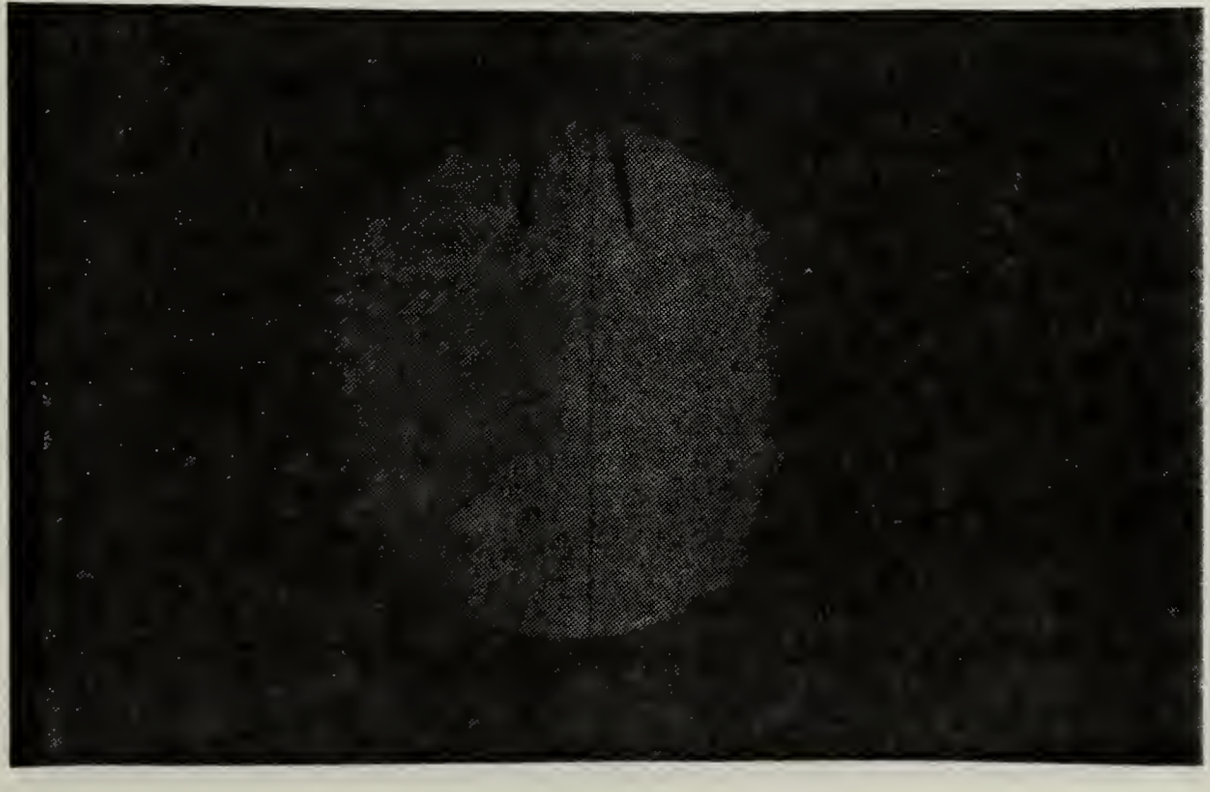

(b)

Figure 6 Sequence of Photographs for Test 3

(c)

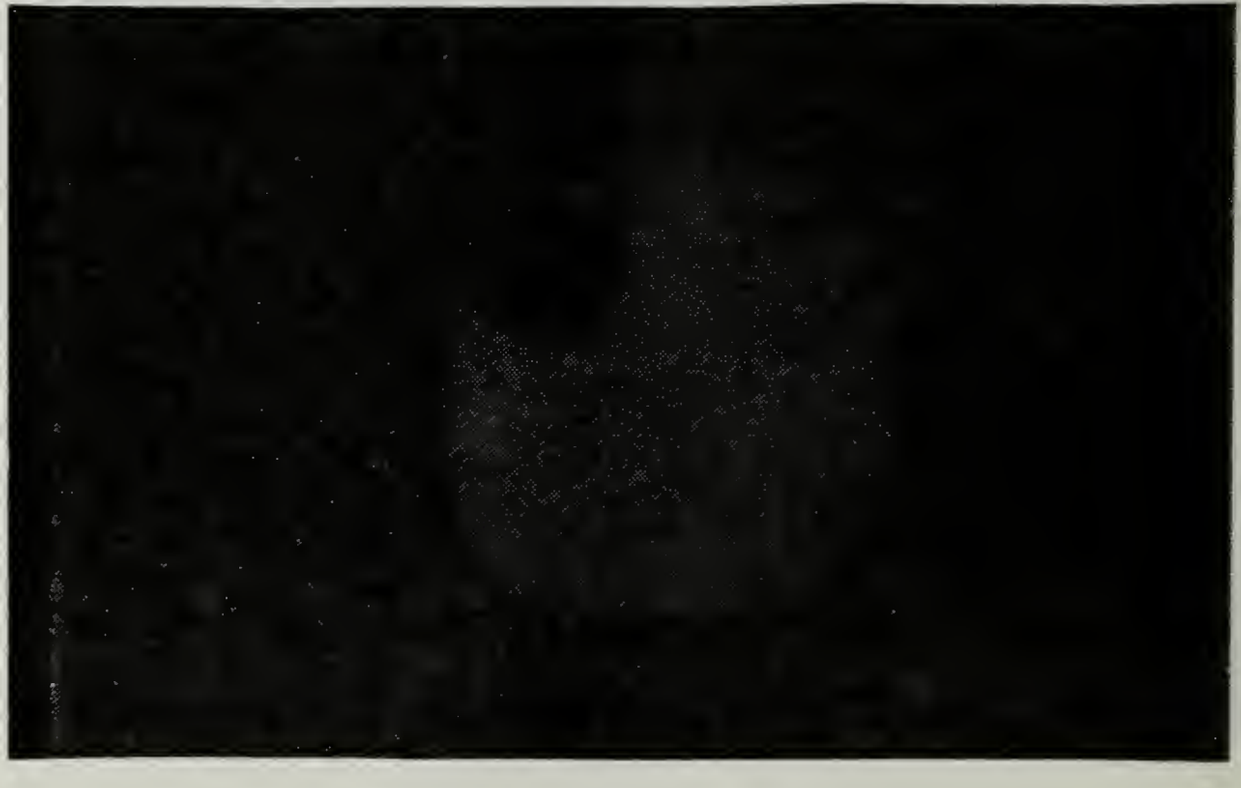

(d)

Figure 6 (Continuation)

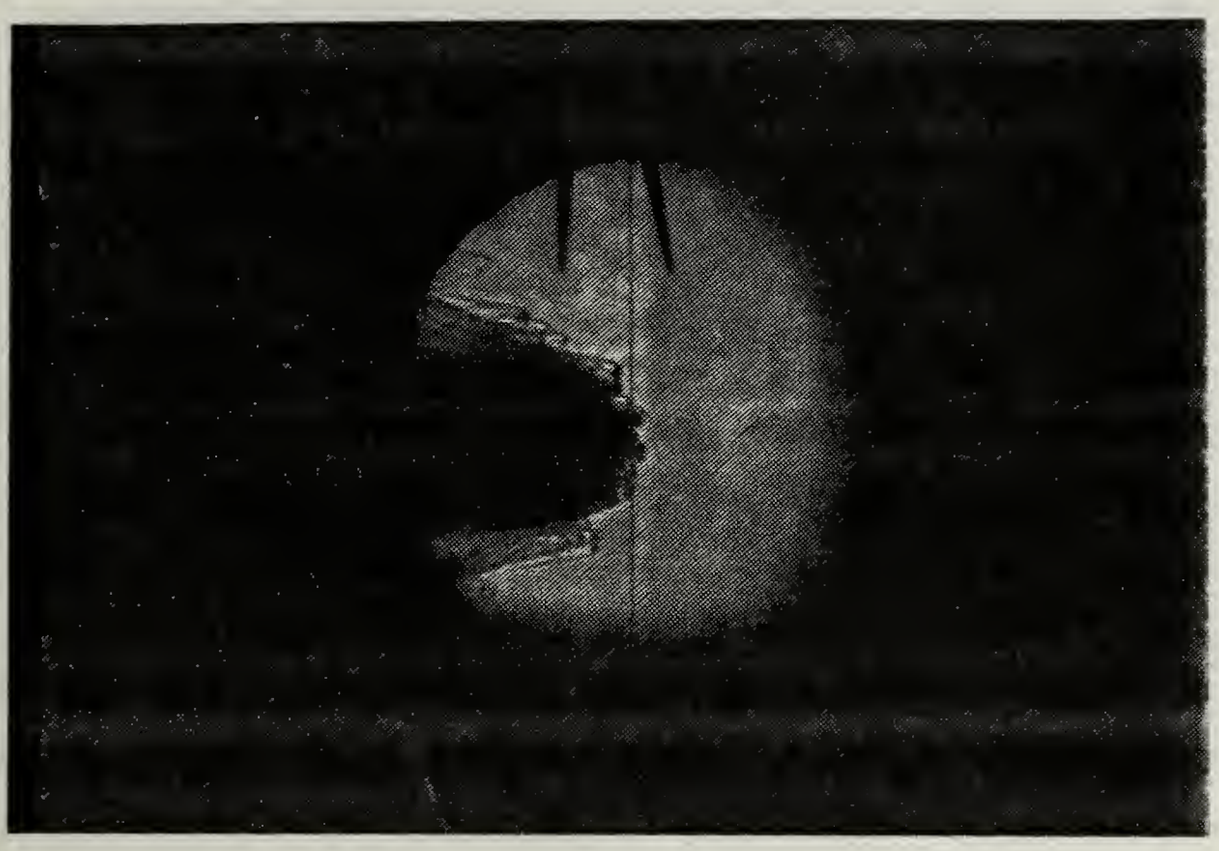

(e)

Figure 6 (Continuation)

process. This does not imply that other types of energy transfer are not taking place. Ablation and other thermodynamic energy transfer may be present. However, for this velocity, observations and study of the photographs indicate that this is not likely to be occurring.

Another point is that, neither the small particles nor the large ones are suffering a combustion process, so the particle size for energy transition from kinetic to chemical is considered to be below the 5 micron size for speeds around 2500 meters per second. Above this speed the

particle may or may not show combustion. Energy transfer of the particles may be accomplished differently.

Figure 7 represents test 4 and shows a series of photographs of the fragment beam alone, well beyond the impact point. The target used was an aluminum plate instead of glass as for the previous tests. The time delay between frames for this sequence is 14.36 microseconds. The bleached and blurred areas that make the fragment beam hard to detect were caused by the luminosity created when the projectile impacted the aluminum target. Close examination of the target plate revealed that the gelatine capsule broke just before impact allowing the particles to be free and transfer some of the kinetic energy to the impact plate.

The impact, created a high enough temperature that started combustion of the aluminum particles. The combusting particles were then carried through by the main fragment beam and are clearly shown in Figure 7e. A piece of cotton string, which was placed as a second reference mark, is undergoing combustion. This is proof that combustion can be observed in the photographs.

Another point that needs to be mentioned is that temperature changes were not obtained for this test; however, the metal to metal impact generated sufficient heat to initiate the combustion process of the aluminum particles. This observation may imply that the total

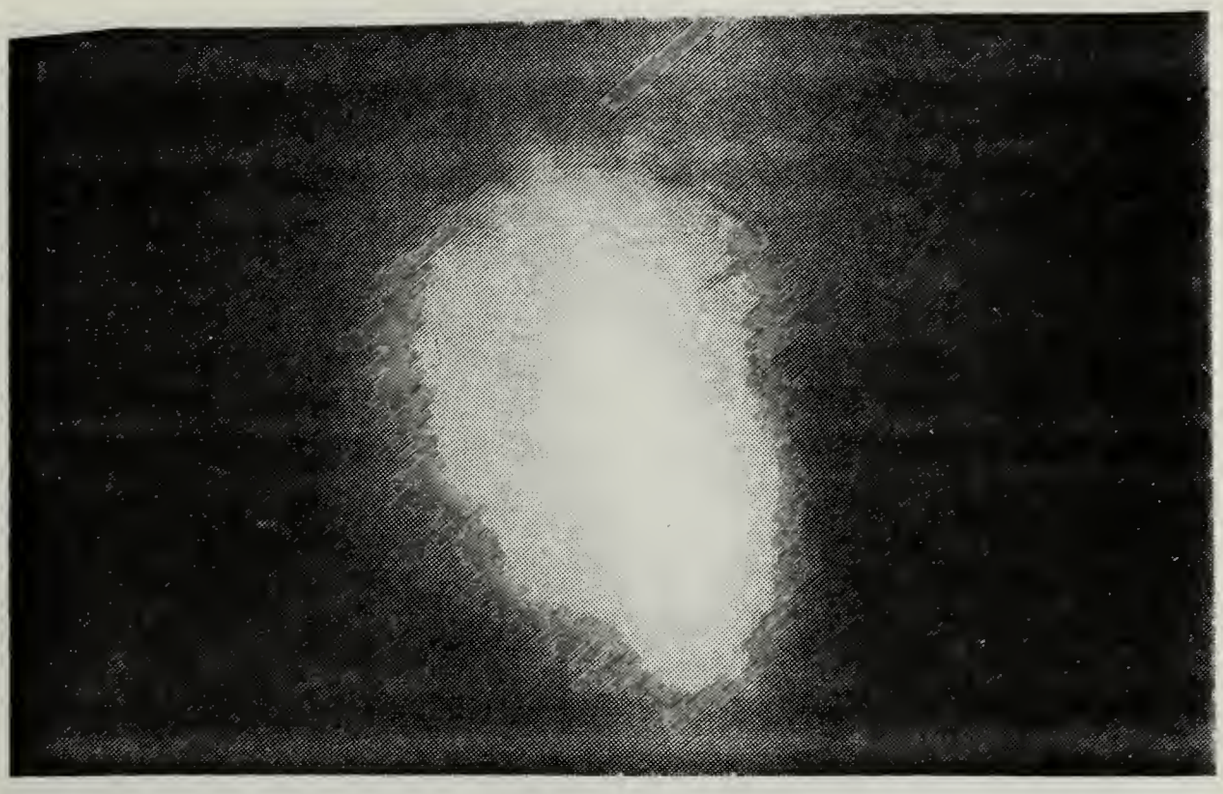

(a)

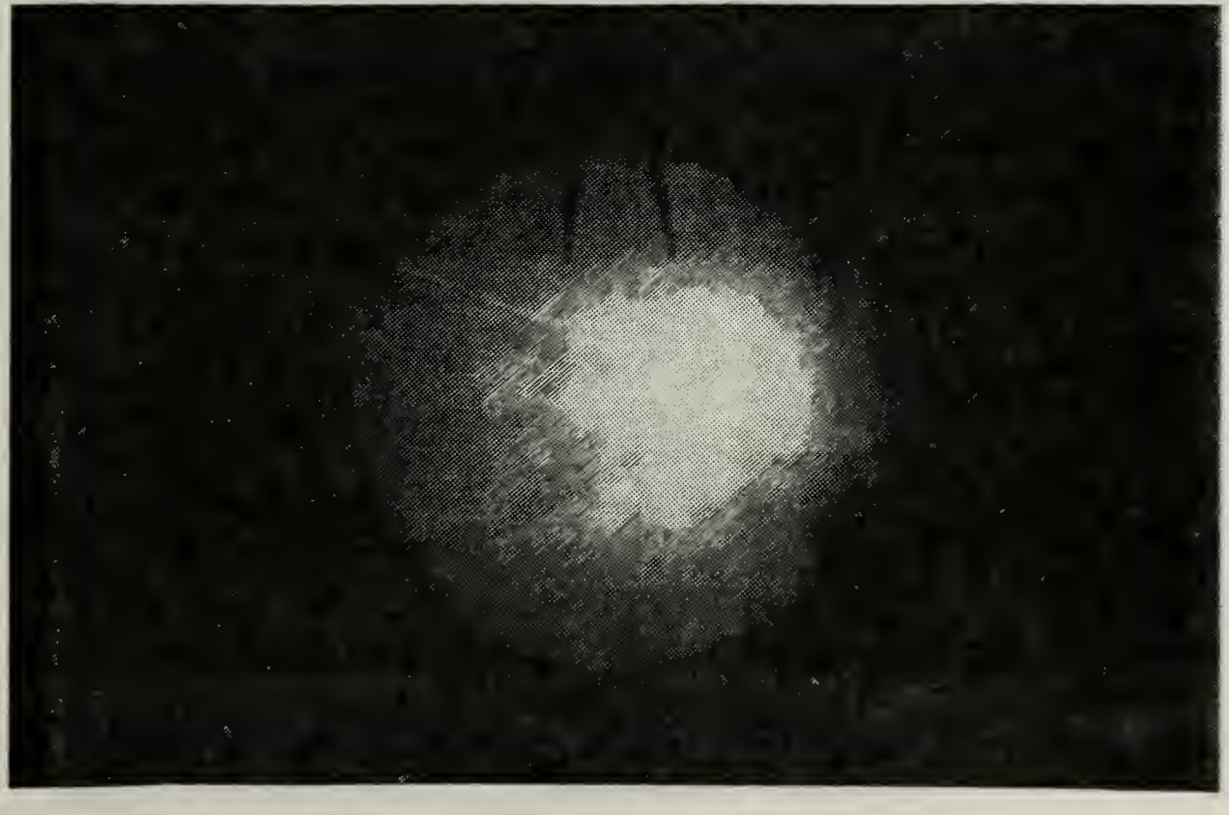

(b)

Figure 7 Sequence of Photographs for Test 4

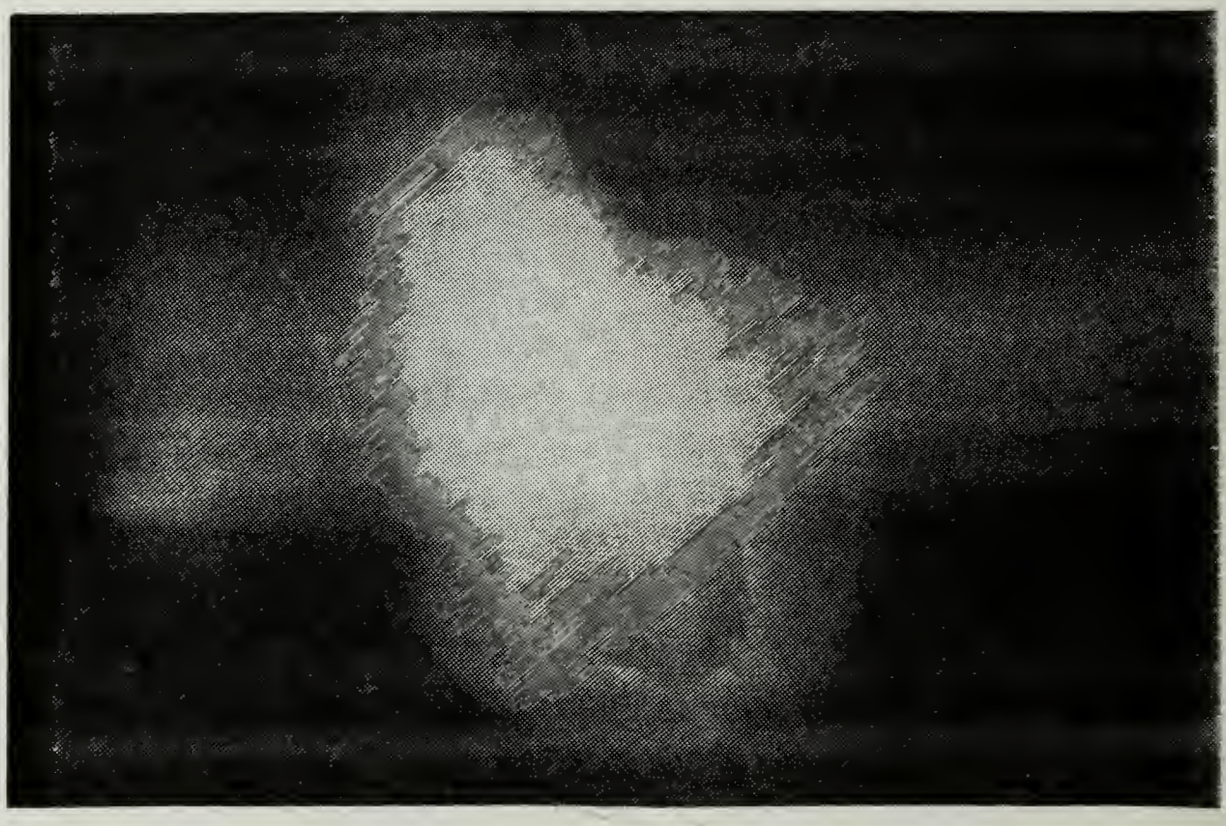

(c)

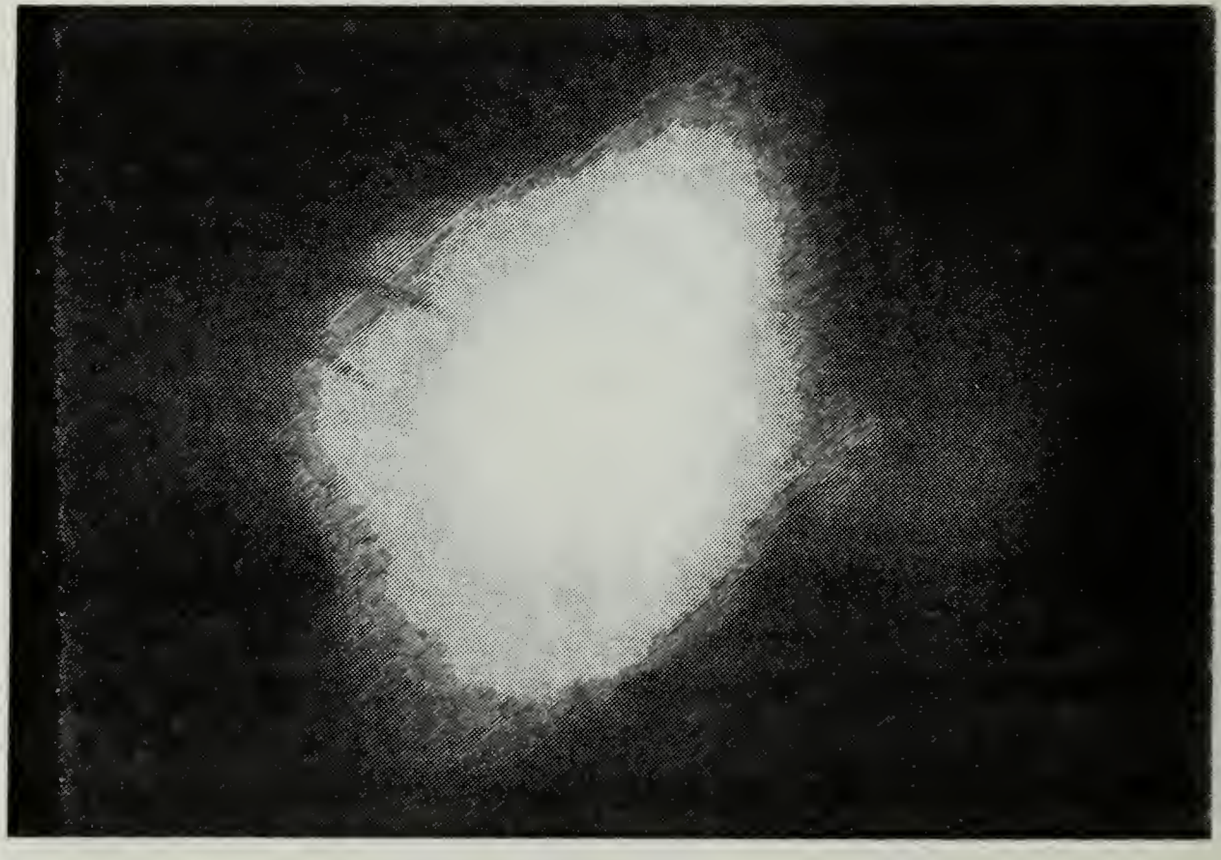

(d)

Figure 7 (Continuation)

(e)

Figure 7 (Continuation)

vaporific effect may be augmented by this impact generated energy.

The witness plates for tests 3 and 4 are shown in Figure 8. They were made of 0.64 centimeter plexiglass board. The particle distribution can easily be studied from these plates since a complete recovery of the plates was possible. Measurements of the fragment beam's radial distribution indicated a diameter of approximately 18.0 to 21.0 centimeters for both plates.

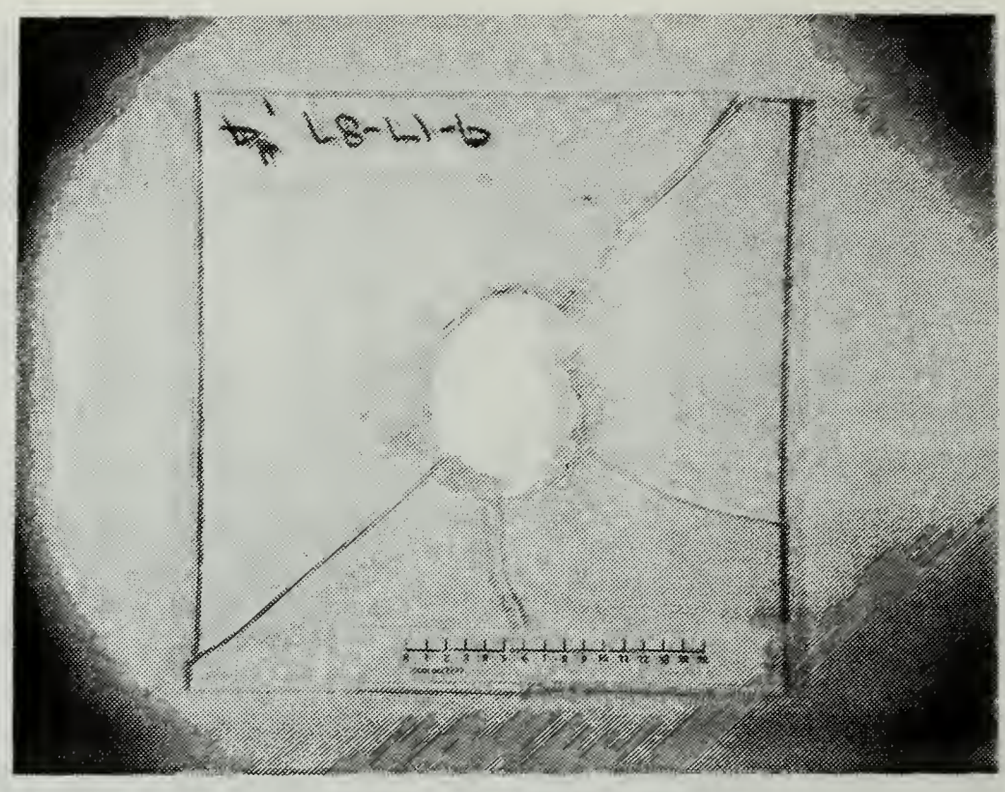

(a)

(b)

Figure 8 Photographs of the Witness Plates for Tests 3 and 4

The witness plate distances behind the target were given in Table I. Distances for tests 3 and 4 were almost three units greater than for tests 1 and 2. Diameter comparisons for tests 1, 2, 3 and 4 indicated that the particle spread remained almost constant despite the different distances traveled by the fragment beam.

The results for test 5 are not presented due to a malfunction of the mechanism that triggers the oscilloscope to record electric signals from the temperature and pressure gauges. The only evidence of this test is a videocassette and a sequence of photographs. The videocassette titled "VAPO EXP 1 and 2", is available by contacting the author of this work. The luminosity generated inside the target produced a complete white out of the photographs, making it impossible to detect the fragment beam or do the analysis of the interaction. The photographs are not contained in this section since no usable data were obtained.

As for test 5, test 6 used a pressure and a temperature gauge. The results of this test are stored in a double sided/double density minidisk used with the oscilloscope. Figure 9 shows a photograph of the signals as viewed from the oscilloscope picture tube. This photograph is a plot of both signals, temperature and pressure, in volts versus time. Readings are in millivolts and microseconds. This test is also included in the videocassette referenced for test number 5.

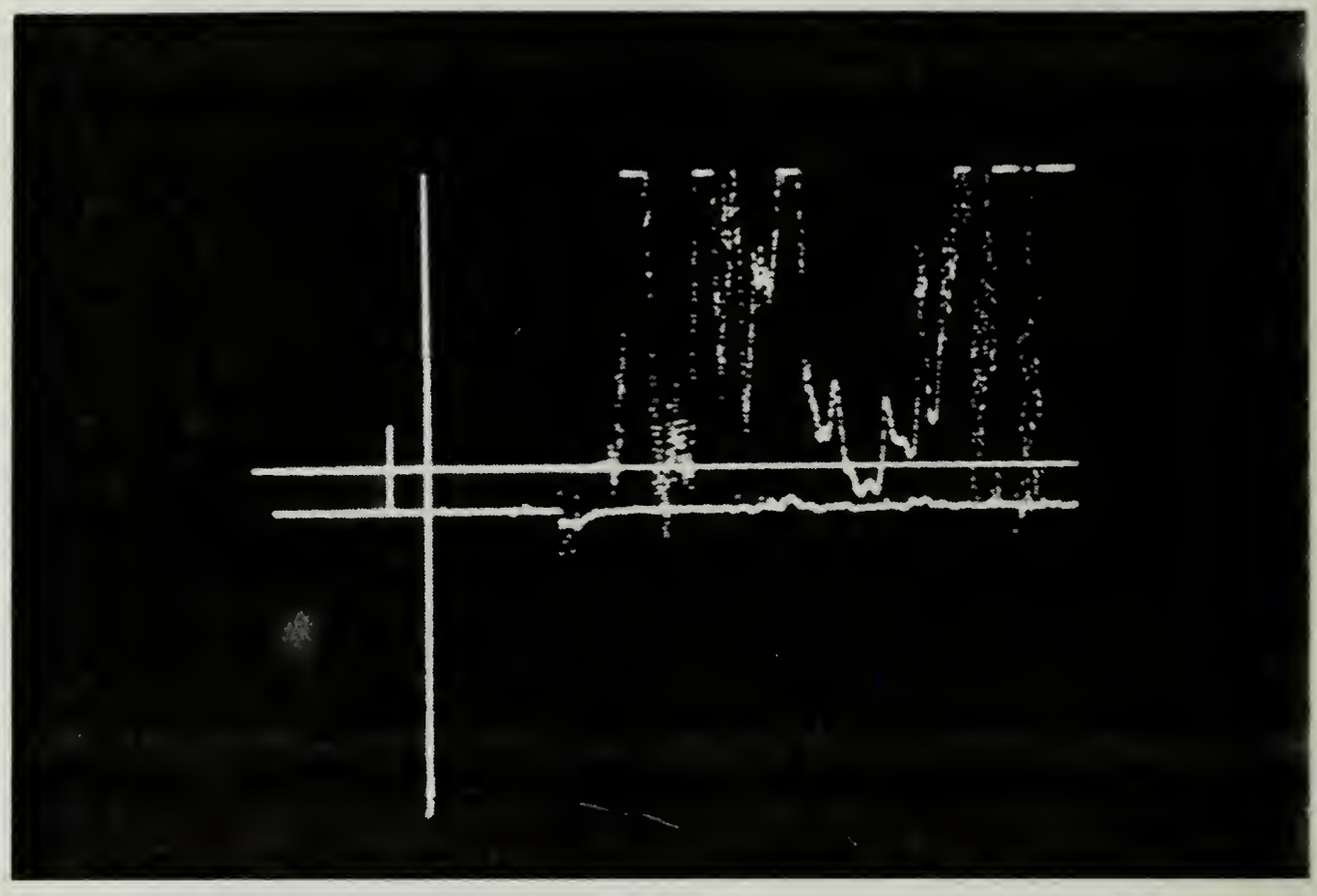

Figure 9 Photograph of the Pressure and Thermocouple Signals as Seen on the Oscilloscope Picture Tube

Figures 10 and 11 are computer enlargements of the individual signals for pressure and temperature. As noticed on both figures a lot of undesired noise accompanied the signals. Figure 10 shows flat areas on the curve. These areas are periods for which the pressure inside the target were far greater than the measuring capabilities of the transducer. They indicate that the transducer reached maximum value. Figure 11 also shows a lot of noise with the signal; however, periods of a definite abrupt change in temperature are readily appreciated.

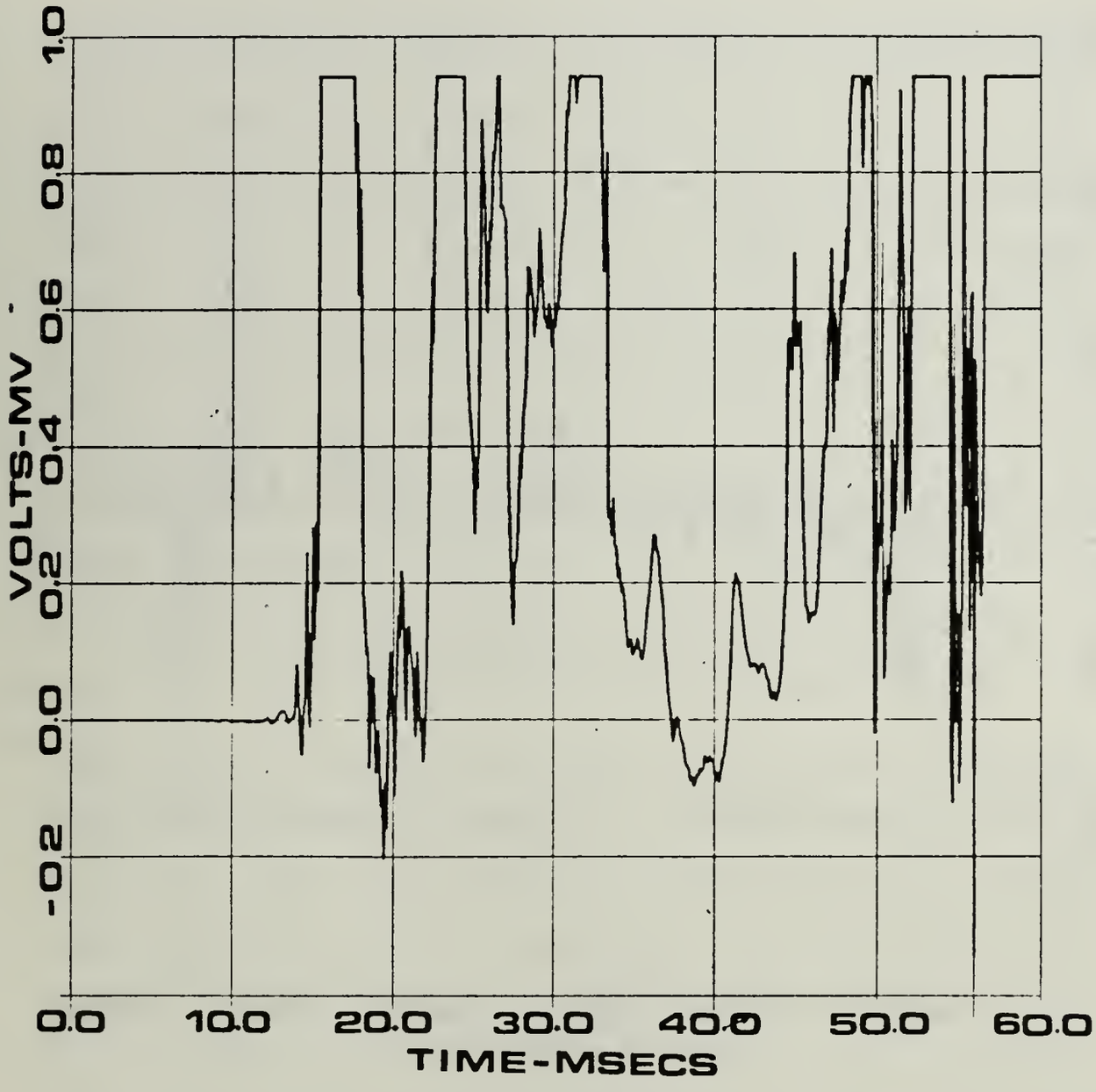

Figure 10 Computer Enlargement of the Pressure Signal

Unfortunately, tests 5 and 6 were designed with the purpose of comparing the temperature and pressure changes for different volume targets. The lack of data obtained from test 5 made this objective impossible to achieve. The study of Figures 10 and 11 and using Appendices A and B, revealed that the pressure increase inside the target

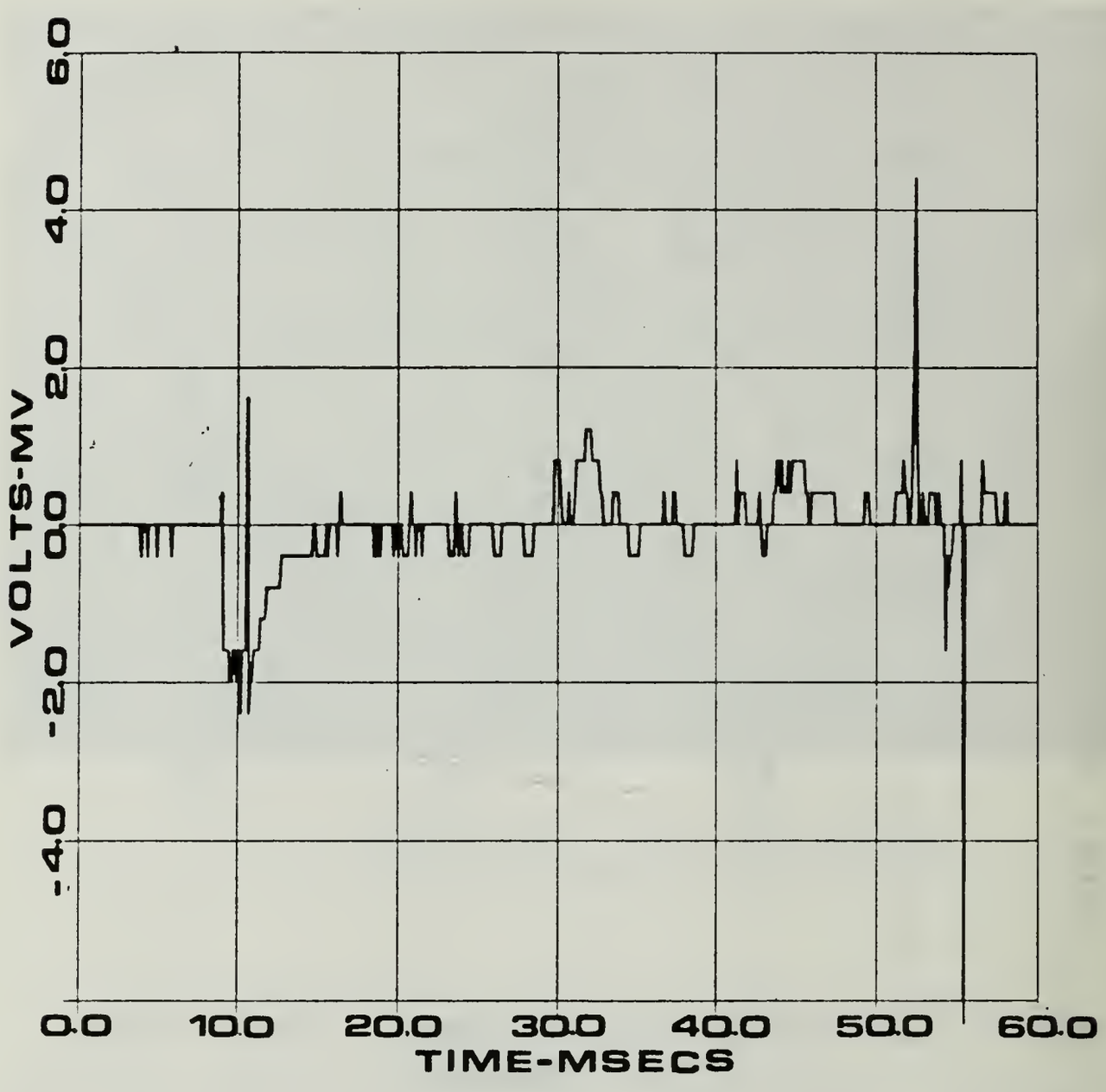

Figure 11 Computer Enlargement of the Thermocouple Signal

exceeded, by a large margin, the rating of the transducer, which was set for 15 PSI. It was estimated that the pressure change was larger than 30 PSI. This is just an estimate and must not be taken as an accurate number.

Temperature changes were determined to increase as much as 100 degrees centigrade. This temperature also contains a degree of inaccuracy, since the thermocouple was not

sensitive enough to register total thermal change in the microsecond range. Taking in consideration the insensitivity of the thermocouple and the fact that changes occurred too fast to be accurately measured, it is assumed that the temperature change inside the target reached well above the 100 degrees recorded.

Figure 12 shows photographs of the back plates of the target boxes. Figure 13 shows magnified photographs of the plates center areas. Analysis of these plates demonstrated that the particle distribution remained almost the same for both tests, even though the distance traveled by the fragment beam was doubled for one of the tests. The same effect was noticed for tests 1, 2, 3 and 4 previously discussed. Also noticed was the large amount of combustion residue left as a yellow film covering the entire area of the plate. This residue is an indication of the large energy transformation taking place inside the compartment. This method of transferring kinetic energy and momentum into heat is believed to be the main cause of the vaporific effect. Furthermore, the crater left by each individual particle provided evidence of total transfer of residual kinetic energy into thermal energy within the target.

The assessment of these plates, supported by the slow and careful study of the videocassette for these tests, indicate that the effects producing the vaporific explosions

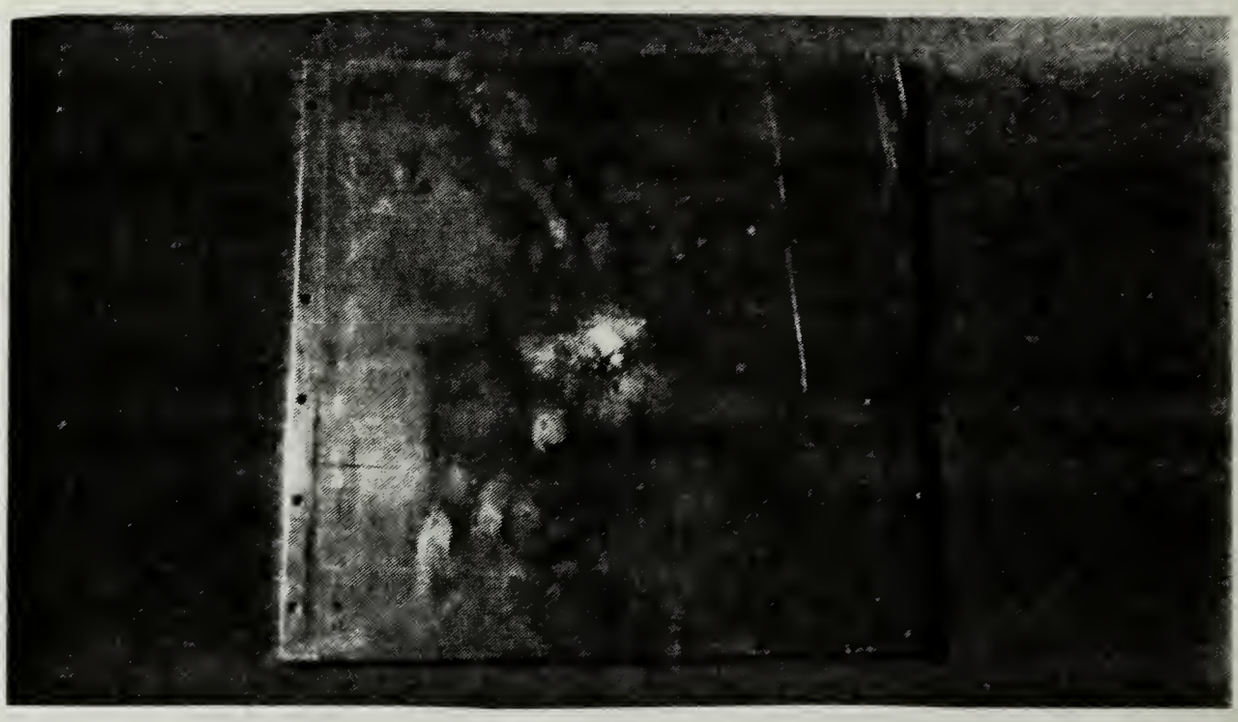

(a)

(b)

Figure 12 Photographs of the Back Plates for Test 5 and 6

(a)

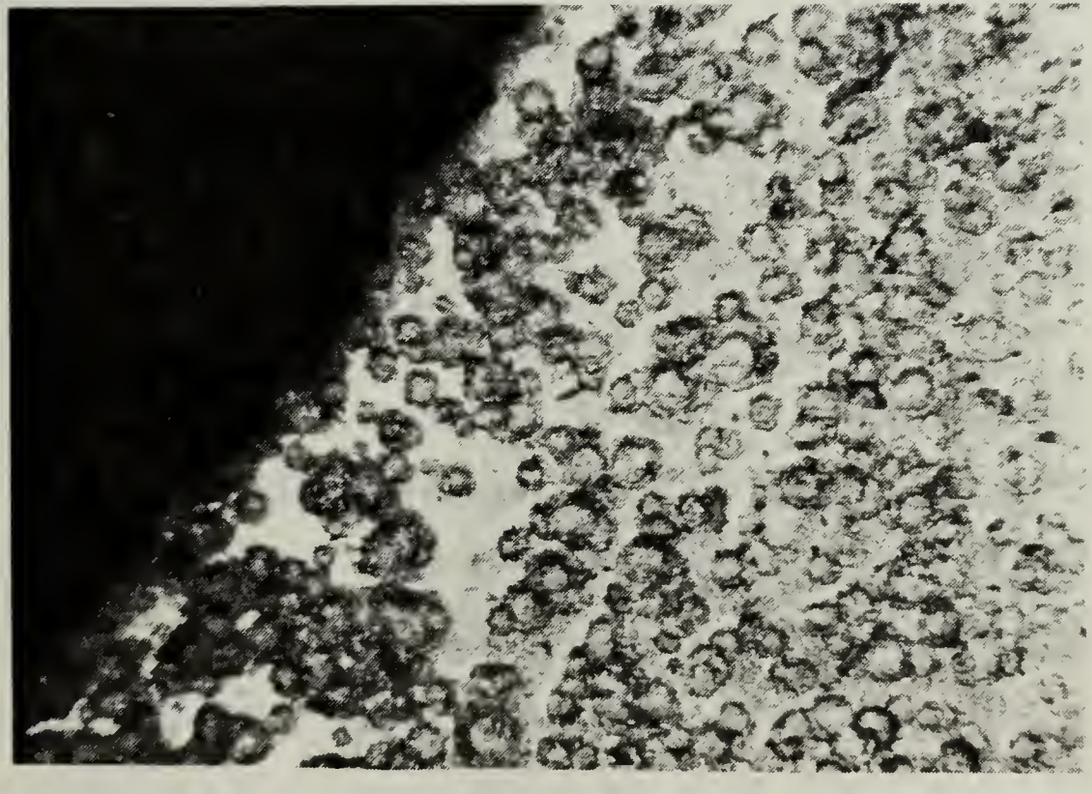

(b)

Figure 13 Photographs of the Magnified Sections of the Back Plates for Tests 5 and 6

are due mainly to the transfer of kinetic energy and momentum of the fragment beam to the interior components of the compartment or target, in our case the back plate. If each individual crater formed is analyzed in terms of how much energy was expended for its formation, and then taking an average of the number of particles in the fragment beam spread over a specific area, an estimate of the total energy dumped into the target can be obtained.

Initially, the particles are contained inside the projectile. They were considered the total mass of the projectile as in a solid. At impact, the particles begin radial distribution. The initial velocity of impact is affected very little. This velocity is maintained by each individual particle. At this point the total kinetic energy remaining, of the original projectile, is now distributed among the particles within the fragment beam. As the fragment beam continues, the particles are decelerated by the air, which takes some energy. However, the residual energy and momentum, originally contained by the projectile, are now distributed over a larger area. Therefore, the disposition and/or transfer of residual energy and momentum is accomplished easily each particle.

VI. CONCLUSIONS AND RECOMMENDATIONS

A. CONCLUSIONS

Based on the results and analysis presented by this experiment, the following can be concluded.

Combustion of the particles within the fragment beam was not observed for speeds below 2500 meters per second; therefore, the transition of events from mechanical (kinetic) energy to chemical (combustion) energy was not observed and are not considered to be the main cause for vaporific explosions. This was noted during the first series of tests and verified by the analysis of the witness plates and back plates of the target boxes. Since the smallest particle size used was 5.0 microns, the critical particle size for which the kinetic energy is transformed into thermal energy is believed to remain under the 5.0 micron range.

Indications are that the most relevant physical principle that contributes the most to the vaporific effect, is the transfer of kinetic energy and momentum of each individual particle of the fragment beam to surfaces in the target. The energy deposited on these surfaces is manifested in the form of heat, which in turn raises the temperature of the surroundings, increasing the pressure. This extremely fast transition phenomenon is manifested as

an explosion. The careful analysis of the target back plates in conjunction with the videocassette study, support this conclusion.

No conclusions were drawn from the tests where a pressure transducer and a thermocouple were used. The tests were performed for the purpose of comparing pressure and temperature changes for compartments of different volume. Unfortunately no data were obtained for the one cubic foot target.

B. RECOMMENDATIONS

Further research on vaporific explosion should continue. Although combustion of the particles was not observed for speeds around 2500 meters per second, working with higher speeds may provide different results.

The particle size should be increased to include diameters equal in magnitude to the target thickness.

Targets, to include large volumes, should be monitored with gauges of very short response time since changes occur in the microsecond range.

A high speed movie camera would greatly enhance the capabilities of analyzing results. A ballistic pendulum can provide very useful data for momentum and impulse analysis.

APPENDIX A

PRESSURE TRANSDUCER HISTORY SHEET

Gage No. 2903 - Calibration History Sheet

DATE	PRESS	mv OUT	SENSITIVITY	DATE	PRESS	mv OUT	SENSITIVITY
6-23-87	120.4	7.760	64.66				
	90	5.890	65.44				
	60	3.915	65.25				
	29.9	1.905	63.71				

APPENDIX B

TEMPERATURE-EMF CONVERSION CHARTS

TABLE VIII

TEMPERATURE-EMF FOR TYPE K THERMOCOUPLES

TEMPERATURES IN DEGREES F.* — REFERENCE JUNCTION AT 32 DEGREES F.

DEG F	0	10	20	30	40	50	60	70	80	90	100	DEG F
					THERMOELECTRIC VOLTAGE IN ABSOLUTE MILLIVOLTS							
-400	-6.344	-6.380	-6.409	-6.431	-6.447	-6.456						-400
-300	-5.632	-5.730	-5.822	-5.908	-5.989	-6.064	-6.133	-6.195	-6.251	-6.301	-6.344	-300
-200	-4.381	-4.527	-4.669	-4.806	-4.939	-5.067	-5.190	-5.308	-5.421	-5.529	-5.632	-200
-100	-2.699	-2.883	-3.065	-3.242	-3.417	-3.587	-3.754	-3.917	-4.075	-4.230	-4.381	-100
- 0	-0.692	-0.904	-1.114	-1.322	-1.527	-1.729	-1.929	-2.126	-2.320	-2.511	-2.699	- 0
+ 0	-0.692	-0.478	-0.262	-0.044	0.176	0.397	0.619	0.843	1.068	1.294	1.520	+ 0
100	1.520	1.748	1.977	2.206	2.436	2.666	2.896	3.127	3.358	3.589	3.819	100
200	3.819	4.049	4.279	4.508	4.737	4.964	5.192	5.418	5.643	5.868	6.092	200
300	6.092	6.316	6.539	6.761	6.984	7.205	7.427	7.649	7.870	8.092	8.314	300
400	8.314	8.537	8.759	8.983	9.206	9.430	9.655	9.880	10.106	10.333	10.560	400
500	10.560	10.787	11.015	11.243	11.472	11.702	11.931	12.161	12.392	12.623	12.854	500
600	12.854	13.085	13.317	13.549	13.781	14.013	14.246	14.479	14.712	14.945	15.178	600
700	15.178	15.412	15.646	15.880	16.114	16.349	16.583	16.818	17.053	17.288	17.523	700
800	17.523	17.759	17.994	18.230	18.466	18.702	18.938	19.174	19.410	19.646	19.883	800
900	19.883	20.120	20.356	20.593	20.830	21.066	21.303	21.540	21.777	22.014	22.251	900
1,000	22.251	22.488	22.725	22.961	23.198	23.435	23.672	23.908	24.145	24.382	24.618	1,000
1,100	24.618	24.854	25.091	25.327	25.563	25.799	26.034	26.270	26.505	26.740	26.975	1,100
1,200	26.975	27.210	27.445	27.679	27.914	28.148	28.382	28.615	28.849	29.082	29.315	1,200
1,300	29.315	29.547	29.780	30.012	30.244	30.475	30.706	30.937	31.168	31.399	31.629	1,300
1,400	31.629	31.859	32.088	32.317	32.546	32.775	33.003	33.231	33.459	33.686	33.913	1,400
1,500	33.913	34.140	34.366	34.593	34.818	35.044	35.269	35.494	35.718	35.942	36.166	1,500
1,600	36.166	36.390	36.613	36.836	37.058	37.280	37.502	37.724	37.945	38.166	38.387	1,600
1,700	38.387	38.607	38.827	39.046	39.266	39.485	39.703	39.922	40.140	40.358	40.575	1,700
1,800	40.575	40.792	41.009	41.225	41.442	41.657	41.873	42.088	42.303	42.518	42.732	1,800
1,900	42.732	42.946	43.159	43.373	43.585	43.798	44.010	44.222	44.434	44.645	44.856	1,900
2,000	44.856	45.066	45.276	45.486	45.695	45.904	46.113	46.321	46.529	46.737	46.944	2,000
2,100	46.944	47.150	47.356	47.562	47.767	47.972	48.177	48.381	48.584	48.787	48.990	2,100
2,200	48.990	49.192	49.394	49.595	49.796	49.996	50.196	50.395	50.594	50.792	50.990	2,200
2,300	50.990	51.187	51.384	51.580	51.776	51.971	52.165	52.360	52.553	52.747	52.939	2,300
2,400	52.939	53.132	53.324	53.515	53.706	53.897	54.087	54.277	54.466	54.656	54.845	2,400
2,500	54.845											2,500
DEG F	0	10	20	30	40	50	60	70	80	90	100	DEG F

* CONVERTED FROM DEGREES C(IPTS 1968).

TABLE VIIIa

CORRECTION TABLE FOR REFERENCE JUNCTION OTHER THAN 32°F

(Correction to be Added to Observed EMF)

TEMPERATURES IN DEGREES F.* — REFERENCE JUNCTION AT 32 DEGREES F.

DEG F	0	1	2	3	4	5	6	7	8	9	10	DEG F
					THERMOELECTRIC VOLTAGE IN ABSOLUTE MILLIVOLTS							
30	-0.044	-0.022	0.000	0.022	0.044	0.066	0.088	0.110	0.132	0.154	0.176	30
40	0.176	0.198	0.220	0.242	0.264	0.286	0.308	0.331	0.353	0.375	0.397	40
50	0.397	0.419	0.441	0.464	0.486	0.508	0.530	0.553	0.575	0.597	0.619	50
60	0.619	0.642	0.664	0.686	0.709	0.731	0.753	0.776	0.798	0.821	0.843	60
70	0.843	0.865	0.888	0.910	0.933	0.955	0.978	1.000	1.023	1.045	1.068	70
80	1.068	1.090	1.113	1.135	1.158	1.181	1.203	1.226	1.248	1.271	1.294	80
90	1.294	1.316	1.339	1.362	1.384	1.407	1.430	1.452	1.475	1.498	1.520	90
100	1.520	1.543	1.566	1.589	1.611	1.634	1.657	1.680	1.703	1.725	1.748	100
110	1.748	1.771	1.794	1.817	1.839	1.862	1.885	1.908	1.931	1.954	1.977	110

APPENDIX B

(CONTINUATION)

TABLE IX

TEMPERATURE-EMF FOR TYPE K THERMOCOUPLES

TEMPERATURES IN DEGREES C (IPTS 1968). REFERENCE JUNCTION AT 0 DEGREES C.

DEG C	0	10	20	30	40	50	60	70	80	90	100	DEG C
					THERMOELECTRIC VOLTAGE IN ABSOLUTE MILLIVOLTS							
-200	-5.891	-6.035	-6.158	-6.262	-6.344	-6.404	-6.441	-6.458				-200
-100	-3.553	-3.852	-4.138	-4.410	-4.669	-4.912	-5.141	-5.354	-5.550	-5.730	-5.891	-100
- 0	0.000	-0.392	-0.777	-1.156	-1.527	-1.889	-2.243	-2.586	-2.920	-3.242	-3.553	- 0
+ 0	0.000	0.397	0.798	1.203	1.611	2.022	2.436	2.850	3.266	3.681	4.095	+ 0
100	4.095	4.508	4.919	5.327	5.733	6.137	6.539	6.939	7.338	7.737	8.137	100
200	8.137	8.537	8.938	9.341	9.745	10.151	10.560	10.969	11.381	11.793	12.207	200
300	12.207	12.623	13.039	13.456	13.874	14.292	14.712	15.132	15.552	15.974	16.395	300
400	16.395	16.818	17.241	17.664	18.088	18.513	18.938	19.363	19.788	20.214	20.640	400
500	20.640	21.066	21.493	21.919	22.346	22.772	23.198	23.624	24.050	24.476	24.902	500
600	24.902	25.327	25.751	26.176	26.599	27.022	27.445	27.867	28.288	28.709	29.128	600
700	29.128	29.547	29.965	30.383	30.799	31.214	31.629	32.042	32.455	32.866	33.277	700
800	33.277	33.686	34.095	34.502	34.909	35.314	35.718	36.121	36.524	36.925	37.325	800
900	37.325	37.724	38.122	38.519	38.915	39.310	39.703	40.096	40.488	40.879	41.269	900
1.000	41.269	41.657	42.045	42.432	42.817	43.202	43.585	43.968	44.349	44.729	45.108	1.000
1.100	45.108	45.486	45.863	46.238	46.612	46.985	47.356	47.726	48.095	48.462	48.828	1.100
1.200	48.828	49.192	49.555	49.916	50.276	50.633	50.990	51.344	51.697	52.049	52.398	1.200
1.300	52.398	52.747	53.093	53.439	53.782	54.125	54.466	54.807				1.300
DEG C	0	10	20	30	40	50	60	70	80	90	100	DEG C

TABLE IXa

CORRECTION TABLE FOR REFERENCE JUNCTION OTHER THAN 0°C

(Correction to be Added to Observed EMF)

TEMPERATURES IN DEGREES C (IPTS 1968). REFERENCE JUNCTION AT 0 DEGREES C.

DEG C	0	1	2	3	4	5	6	7	8	9	10	DEG C
						THERMOELECTRIC VOLTAGE IN ABSOLUTE MILLIVOLTS						
0	0.000	0.039	0.079	0.119	0.158	0.198	0.238	0.277	0.317	0.357	0.397	0
10	0.397	0.437	0.477	0.517	0.557	0.597	0.637	0.677	0.718	0.758	0.798	10
20	0.798	0.838	0.879	0.919	0.960	1.000	1.041	1.081	1.122	1.162	1.203	20
30	1.203	1.244	1.285	1.325	1.366	1.407	1.448	1.489	1.529	1.570	1.611	30
40	1.611	1.652	1.693	1.734	1.776	1.817	1.858	1.899	1.940	1.981	2.022	40

LIST OF REFERENCES

1. The New Mexico School of Mines, Albuquerque, New Mexico, The Effectiveness of 1/4 Inch Steel Cubes in Damaging Aircraft, by Morgan G. Smith and John S. Rinehart, 3 December 1947.

2. U. S. Naval Ordnance Test Station, China Lake, California, NOTS 1113, NAVORD Report 3490, The Mechanism of Vaporific Damage to Aircraft Structures, by Terry Triffet, 14 June 1955.

3. U. S. Naval Ordnance Test Station, China Lake, California, NOTS TP 2093, NAVORD Report 6398, Semi-Quantitative Analysis of Shape Charge Vaporific Damage, by L. N. Cosner, R. G. S. Sewell, and H. W. Wedaa, 18 September 1958.

4. U. S. Naval Ordnance Test Station, China Lake, California, NOTS 672, NAVORD Report 2018, Studies of Damage to Aircraft Structures by Shape Charges at Long Standoff, by D. R. Kennedy, R. D. Smith, G. C. Throner, and R. G. Wagenseller, 17 March 1953.

5. U. S. Naval Ordnance Test Station, China Lake, California, NOTS TP 2494, NAVWEPS Report 7083, The Cross Wind Firing of Large Shape Charges, by L. N. Cosner and J. Pearson, 3 June 1960.

6. Naval Weapons Center, China Lake, California, NWC TP 6058, Interaction of Multiple Fragment Systems With Plate Array Targets, by M. A. Alexander and S. A. Finnegan, January 1979.

7. Naval Weapons Center, China Lake, California, NWC TP 6089, Peak Overpressures or Internal Blast, by G. G. Kinney, R. G. S. Sewell, and K. J. Graham, June 1979.

8. Naval Weapons Center, China Lake, California, NWC TP 4654 Engineering Elements of Explosions, by G. F. Kinney, November 1968.

9. Kinney, G. F. and Graham, K. J., Explosive Shocks in Air, 2d ed., Springer-Verlag Inc., 1985.

10. Rinehart, J. S., Allen, W. A., and White, W. C., "Phenomena Associated With The Flight of Ultra-Speed Pellets", Journal of Applied Physics, Vol. 23, No. 3, January 1952.

11. Naval Weapons Center, China Lake, California, NWC TP 5780, Terminal Ballistic, by M. E. Backman, February 1976.

12. Naval Weapons Center, China Lake, California, NWC TP 4414, Penetration Mechanics and Post-Perforation Effects in an Aluminum-Aluminum Impact System, by M. E. Backman and W. J. Stronge, October 1967.

INITIAL DISTRIBUTION LIST

		No. Copies
1.	Defense Technical Information Center Cameron Station Alexandria, Virginia 22304-6145	2
2.	Library, Code 0142 Naval Postgraduate School Monterey, California 93943-5002	2
3.	Professor Gilbert F. Kinney Physics Department Code 61KY Naval Postgraduate School Monterey, California 93943	3
4.	Mr. Mark Alexander Code 3894 Naval Weapons Center China Lake, California 93555-6001	1
5.	Mr. Steve Finnegan Code 3894 Naval Weapons Center China Lake, California 93555-6001	1
6.	Mr. Kenneth Pringle Code 3894 Naval Weapons Center China Lake, California 93555-6001	1
7.	Mr. Raimundo Lamboy 2980 Coral Court Jacksonville, Florida 32205	1
8.	CPT Gilberto Rodriguez 2980 Coral Court Jacksonville, Florida 32205	3
9.	Mr. Longino Rodriguez H.C. 72 Box 6574 Cayey, Puerto Rico 00633-9510	1

10. Professor Alan B. Coppens 1
Physics Department Code 61CZ
Naval Postgraduate School
Monterey, California 93943

Thesis
R6727
c.1

Rodriguez
Mechnical-chemical
energy transfer observa-
tions of vaporific explo-
sions.